Radial glia control microglial differentiation via integrin avb8-dependent trans-activation of TGFB1

Gabriel L. McKinsey[1*], Nicolas Santander[2], Xiaoming Zhang[3], Killian Kleeman[3], Aditya Katewa[1], Lauren Tran[1], Kaylynn Conant[1], Matthew Barraza[4], Carlos Lizama[5], Hyun Ji Koo[1], Hyunji Lee[1], Dibyanti Mukherjee[1], Helena Paidassi[6], E. S. Anton[7], Kamran Atabai[5], Dean Sheppard[5], Oleg Butovsky[3], Thomas D. Arnold[1*].

[1]University of California San Francisco, Department of Pediatrics and Newborn Brain Research Institute, San Francisco, CA, USA

[2]Instituto de Ciencias de la Salud, Universidad de O´Higgins, Rancagua, Chile

[3]Ann Romney Center for Neurologic Diseases, Department of Neurology, Brigham and Women's Hospital, Harvard Medical School, Boston, MA, USA

[4]Northwestern University, Department of Neuroscience, Chicago, IL, USA

[5]University of California San Francisco, Cardiovascular Research Institute, San Francisco, CA, USA

[6]Centre International de Recherche en Infectiologie, Lyon, France

[7]University of North Carolina at Chapel Hill, Chapel Hill, NC, USA

*Correspondence: gabriel.mckinsey@ucsf.edu, thomas.arnold@ucsf.edu

Abstract

Microglia diversity emerges from interactions between intrinsic genetic programs and environment-derived signals, but how these processes unfold and interact in the developing brain remains unclear. Here, we show that radial glia progenitor-expressed integrin beta 8 activates microglia-expressed TGFB1, permitting microglial development. Domain-restricted deletion of *Itgb8* in these progenitors establishes complementary domains of developmentally arrested "dysmature" microglia and homeostatic microglia that persist into adulthood. In the absence of autocrine TGFB1 signaling, we find that microglia adopt a similar reactive microglial phenotype, leading to astrogliosis and neuromotor symptoms almost identical to *Itgb8* mutant mice. By comparing mice with genetic deletions in critical components downstream of *Itgb8*, we show that non-canonical (Smad-independent) signaling partially suppresses the dysmature microglia phenotype, associated neuromotor dysfunction and expression of disease-associated genes, providing compelling evidence for the adoption of microglial developmental signaling pathways in the context of injury or disease.

Introduction

A substantial body of evidence has shown that transforming growth factor beta (TGFβ) signaling is crucial for microglial development and function[1]. *In vitro* studies have indicated that microglial-specific gene expression and survival can be induced by application of TGFB[1,2] and *Tgfb1* null mice display severe neuropathological changes, including microgliosis, neuronal cell death, and synaptic loss[3,4]. Mice mutant for the microglial enriched gene *Lrrc33* (*Nrros*), which binds and presents TGFB1 to its cognate receptor TGFBR2, have severe microglial defects, but no major vascular abnormalities[5,6]. These findings suggest that the microglial defects seen in *Tgfb1* mutants are not the result of vascular defects, but rather derive from the direct effects of TGFB1 signaling in microglia. Similarly, conditional deletion of *Tgfbr2* in microglia results in the disruption of microglial homeostasis[7–9].

TGFB1 is synthesized in a latent inactive complex that requires two key steps to be activated[10,11]. First, latent TGFB1 is anchored to the surface of one cell type by a so-called "milieu" molecule, LRRC33 (NRROS). Second, the integrin avb8 dimer on neighboring cells binds to and activates latent-TGFB1, which can then signal to TGFBR2. Cryo-EM analyses of avb8 in complex with TGFB1 and LRRC33 support a model whereby the release and diffusion of active TGFB ligand is not necessary; rather, TGFB1 is positioned by LRRC33 and avb8 to interact with TGFBR2, reinforcing TGFβ signaling in the cell which expresses TGFB1[10,11]. This "paracrine activation / autocrine signaling" model predicts that deletion of *Itgb8* in one cell type primarily effects a neighboring cell type which both presents and responds to TGFB1. Consistent with this model, *Itgb8*, *Tgfb1*, *Tgfb1RGE*, *Lrrc33* mouse mutants have largely overlapping phenotypes. However, the specific cell types expressing these various signaling components, and the timing of their interactions during brain development have remained unclear.

In a previous study, we demonstrated a critical role for integrin avb8 in presenting active TGFβ to microglia[7]. We found that in the absence of avb8-mediated TGFβ signaling, microglia are developmentally arrested and hyper-reactive. Furthermore, the presence of these "dysmature" microglia (and not just the absence of mature microglia) causes loss of GABAergic interneurons and myelination failure, aspects of pathology underlying the development of a severe neuromotor syndrome characterized by seizures and spasticity. We found that this phenotype is entirely due to loss of TGFβ signaling in microglia during brain development because microglia-specific deletion of *Tgfbr2* during early stages of brain development completely recapitulated the *Itgb8* mutant phenotype.

In this study, we aimed to identify 1) The relevant *Itgb8* expressing cell types that mediate microglial TGFβ activation; 2) The developmental timing of *Itgb8*-mediated TGFβ signaling in microglia; 3) The cellular source and identity of the TGFβ ligand relevant for microglial development and homeostasis; 4) The relationship between developmentally disrupted microglia and disease associated microglia, and 5) The role of canonical (Smad-mediated) versus non-canonical TGFβ signaling in microglia. Here, we have defined the genes, timing, and cell-cell interactions required for *Itgb8*-TGFβ dependent development of the neuroimmune system. By systematically deleting *Itgb8* from different cell lineages of the adult and embryonic brain, we show that *Itgb8* expression, specifically in embryonic radial progenitors, is necessary for microglial differentiation, but is dispensable to maintain homeostasis. We find that microglial expressed *Tgfb1* is required cell-autonomously for microglial differentiation and, in contrast to *Itgb8*, is also required for the maintenance of microglial homeostasis. By analyzing various *Itgb8-TGFβ* pathway mutants, we find that non-canonical TGFβ signaling fine-tunes microglial maturation and homeostasis, such that upstream mutants have amplified microglia and neuromotor phenotypes compared to *Smad2/3* conditional mutants. Together, these data support the model that *Itgb8-TGFB1* signaling via radial glia-microglial interactions is crucial for the embryonic maturation of microglia, and that postnatal microglial *Tgfb1* expression is necessary for the maintenance of microglial homeostasis.

Radial glia *Itgb8* expression promotes vascular and microglial development

We previously found that CNS-wide deletion of *Itgb8* using *Nestin^{Cre}* leads to microglial dysmaturation and associated neuromotor impairments nearly identical to those seen in mice with conditional deletion of *Tgfbr2* in microglia[7]. *Nestin^{Cre}* constitutively removes *Itgb8* from all cells derived from the early neuroepithelium (astrocytes, oligodendrocytes, and neurons), and *Itgb8* is expressed in all of these cell types (Supplementary Fig 1)[12]. To determine which of these *Itgb8*-expressing cells are responsible for the phenotypes observed in *Itgb8$^{f/f}$;Nestin^{Cre}* mice, we generated six different *Itgb8* conditional knockout lines to systematically delete *Itgb8* from astrocytes, oligodendrocytes or neurons individually and in combination (Supplementary Figure 2). As summarized in Supplementary Figure 1, none of these cell-type specific *Itgb8* mutants produced the phenotypes observed in *Itgb8$^{f/f}$;Nestin^{Cre}* mice (motor dysfunction, microglial TMEM119/P2RY12 loss, GFAP upregulation) . Most notably, conditional deletion of *Itgb8* using *hGFAP^{Cre}* resulted in no obvious neuropathological changes despite recombining nearly all neuron, astrocytes and oligodendrocytes in the cortex (98.3+/-.3%; 98.1+/-2.7%; 100% respectively)(Supplemental Figure 2). These data indicate that *Itgb8* is dispensable for maintaining microglial, neuro/glial and vascular homeostasis in adult mice.

To understand why *Nestin^{Cre}* mediated *Itgb8* deletion resulted in a fulminant neuromotor phenotype, while deletion from all other brain cell types (alone or in combination) did not, we considered the unique features of *Nestin^{Cre}*[12]. *Nestin^{Cre}*-mediated recombination occurs at ~ embryonic day E10.5, resulting in loss of *Itgb8* in radial

glia and their progeny; Figure 1C,D, Supplementary Figure 2). Interestingly, *hGFAP*^{Cre} also recombines radial glia progenitors and their progeny, but three days later than *Nestin*^{Cre} at ~E13.5[13,14]. Both of these lines have recombination in almost all neurons and glia by adulthood (Supplementary Figure 2). The sequential recombination of brain progenitors in *Itgb8*$^{f/f}$*;Nestin*^{Cre} (complete phenotype) and *Itgb8*$^{f/f}$*;hGFAP*^{Cre} (no apparent phenotype) suggests that the developmental timing of *Itgb8* expression in, or deletion from, neuroepithelial progenitor cells or radial glia is responsible for the stark phenotypic differences in these mice.

Published RNA-Seq (Fig. 1A, Supplemental Figure 3A) and in situ hybridization (Supplemental Figure 3B) show that *Itgb8* is expressed in neuroepithelial progenitor cells throughout the brain starting by E8.5, and that by E14.5 *Itgb8* is most highly expressed in radial glia progenitors, and less so in maturing astrocytes and oligodendrocytes [15]. We confirmed this using *Itgb8*^{tdT} reporter mice, finding intense tdT expression in ventricular zone progenitors at E14.5 (Fig 1b and Supplementary Figure 3C)[16] as well as tdT expression in radial glia fibers and endfeet in the embryonic meninges (open and closed arrowheads in B respectively).

To more directly test the hypothesis that early developmental expression of *Itgb8* is necessary for microglial maturation, we analyzed *Itgb8* conditional knockouts (*Nestin*^{Cre}, *hGFAP*^{Cre}, *Olig2*^{Cre}) at E14.5. We also generated *Itgb8*$^{f/f}$*;Emx1*^{Cre} mice, in which Cre is expressed in neocortical neuroepithelial cells just before the formation of radial glia at E9[17]. As we previously reported[7], we found that *Itgb8*$^{f/f}$*;Nestin*^{Cre} mice develop vascular dysplasia and hemorrhage in the brain starting at E11.5 (not shown), which progresses in a ventral-dorsal fashion to include all periventricular vessels by E14.5 (Fig. 1D). Coinciding with these vascular changes, we observed that IBA1+ macrophages were strongly associated with dysplastic vessels in *Itgb8*$^{f/f}$*;Nestin*^{Cre} mutants (arrowhead in Fig. 1D), and were characteristically dysmature, i.e. lacking expression of mature/homeostatic microglia marker P2RY12, and reciprocally upregulating (or persistently expressing) CD206, a marker of undifferentiated microglial precursors and border associated macrophages (BAMs) (Fig. 1D) [18,19,20,21]. While the vascular phenotype and hemorrhage was largely localized to areas near the cerebral ventricles (the periventricular vascular plexus, PVP), we observed microglia lacking P2RY12 staining throughout the brain, including areas far from hemorrhage, suggesting that the two phenotypes might be dissociable, i.e. that hemorrhage is not causing these widespread microglial changes or vice-versa.

Similar to *Itgb8*$^{f/f}$*;Nestin*^{Cre} embryos, *Itgb8*$^{f/f}$*;Emx1*^{Cre} E14.5 embryos had vascular abnormalities and hemorrhage near the cerebral ventricles, concomitant with microglial changes throughout the developing cortex and hippocampus. However, these vascular/hemorrhage and microglial abnormalities in *Itgb8*$^{f/f}$*;Emx1*^{Cre} mice were strikingly domain-specific; hemorrhage and microglial changes occurred only in regions where Cre-recombinase had been active (as indicated by tdTomato Cre-reporter expression) (Fig. 1D). In sharp contrast, *Itgb8*$^{f/f}$*;hGFAP*^{Cre} mice lacked any apparent phenotype (Fig. 1D). Similar to *Itgb8*$^{f/f}$*;hGFAP*^{Cre} mice, we observed no obvious vascular or microglial phenotype in *Itgb8*$^{f/f}$*;Olig2*^{Cre} (Supplementary Figure 4) . This Cre line is active at or before E14.5, but not in radial glia. Based on the timing of *Itgb8* expression in the brain and the timing of recombination in these various Cre lines (*Emx1*^{Cre} ~E9; *Nestin*^{Cre} ~E10.5; *hGFAP*^{Cre} ~E13.5), our data indicate that *Itgb8* expression in early stage radial progenitors promotes both vascular and microglia maturation, and that expression of *Itgb8* in astrocytes, oligodendrocytes, and in post-mitotic neurons is dispensable for brain vascular and microglia development, and for ongoing cellular homeostasis.

Initial descriptions of microglia by del Rio-Hortega proposed that microglia are developmentally derived from the inner layer of the meninges, the pia mater[22]. Recent genetic fate-mapping reports show that microglia are derived from a CD206 expressing undifferentiated macrophage precursor[21,19,20].Upon differentiating, these progenitors down-regulate the expression of CD206 and up-regulate microglial markers such as P2RY12. To determine whether embryonic radial glia make contact with CD206+ microglial precursors, we crossed *Emx1*^{Cre} mice to a mouse line (*RG-Brainbow*) that mosaicly expresses a Cre-dependent plasma membrane-tagged fluorescent reporter under the GLAST promotor[23]. We then examined the interaction between radial glial endfeet and CD206+ macrophages in the meninges, where most embryonic CNS-associated CD206+ macrophages reside. Analysis of the mosaic expression of mGFP (membranous) in E14.5 *Emx1*^{Cre}*;RG-Brainbow* embryos revealed contact between radial glia endfeet and CD206+ macrophages in the innermost layer of the meninges (Figure 1G), consistent with the model that meningeal CD206+ microglial precursor interaction with *Itgb8* expressing radial glial endfeet is necessary for the TGFβ-dependent differentiation of these progenitors (Figure 1H).

In total, these data suggest that *Itgb8* expression in early embryonic radial glia is necessary for the TGFβ-dependent differentiation of CD206+ microglial precursors, and that in the absence of *Itgb8*, these CD206+ precursors populate the brain, but fail to express microglial-specific markers.

Domain-specific microglial dysmaturation persists in adult *Itgb8$^{f/f}$;Emx1^{Cre}* mice

We next followed *Itgb8$^{f/f}$;Emx1^{Cre}* mice into adulthood to see how developmental phenotypes might evolve over time. Similar to *Itgb8$^{f/f}$;Nestin^{Cre}*, mice, vascular defects and hemorrhage resolved, while microglial changes persisted. To examine the transcriptional properties of microglia in *Itgb8$^{f/f}$;Emx1^{Cre}* mice, we isolated affected cortical and hippocampal microglia microglia by fluorescence-activated cell sorting and sequenced RNA derived from these microglia. To explore our hypothesis that cortical and hippocampal microglia in *Itgb8$^{f/f}$;Emx1^{Cre}* microglia are developmentaly blocked in an immature state, we compared this transcriptional data to a recently published trancriptional analysis that identified 7 clusters of genes associated with microglia at various stages of development, from the early yolk sac progenitor stage through embryonic development and into adulthood[24]. Remarkably, when we compared the expression of these genes in adult *Itgb8$^{f/f}$;Emx1^{Cre}* dysmature microglia to adult control microglia, we found a striking enrichment for genes in clusters 3-5, which represent transcripts that are enriched in microglia during early development (Figure 2A, B). Conversely, genes that were enriched in clusters 6 and 7, which represent late embryonic/neonatal and adult stages were strikingly downregulated (Fig. 2B). Immunohistochemical analysis revealed that the dysmature microglia phenotype was identical to that we observed in *Itgb8$^{f/f}$;Nestin^{Cre}*, and *Tgfbr2$^{f/f}$;Cx3cr1^{Cre}* mice (P2RY12^{neg}, Tmem119^{neg}; CD206^{hi}, CLEC7a^{hi} and APOE^{hi}) and was tightly restricted to the *Emx1^{Cre}* recombination domain (Figure 2C-G). Outside this domain, microglia were comparable to control mice. Surprisingly, and in contrast to *Itgb8$^{f/f}$;Nestin^{Cre}*, mice, *Itgb8$^{f/f}$;Emx1^{Cre} mice* had no obvious neuro-motor deficits or early mortality, suggesting that the profound motor disturbances in *Itgb8$^{f/f}$;Nestin^{Cre}* and *Tgfbr2$^{f/f}$;Cx3cr1^{Cre}* are not derived from disruption of the motor or sensory cortex.

We also observed that among the genes enriched in dysmature *Itgb8$^{f/f}$;Emx1^{Cre}* microglia, a number of these genes are also enriched in disease and injury states (Fig. 2A, H). Furthermore, many of these disease and injury-associated genes are developmentally expressed (Fig. 2A), suggesting that disease and injury-associated microglia recapitulate transcriptional states associated with progenitor and early embryonic developmental stages. Together, these experiments indicate that domain-specific deletion of *Itgb8* results in the blockage of microglial development, leaving them trapped in an early embryonic progenotor state, and establishes complementary domains of microglial dysmaturation and homeostasis that are maintained into adulthood.

***Tgfb1* is required cell-autonomously for microglial development**

The only known biological function of ITGB8 is to activate TGFB1 and TGFB3[10,11] and *Tgfb1$^{-/-}$* mutant mice display neuropathology that closely resembles the various neurovascular and neuroimmune phenotypes observed in *Nestin^{Cre}* and *Emx1^{Cre};Itgb8$^{f/f}$* conditional mutants[4]. Recent structural biology studies[10,11] reveal a mechanism of TGFB1 activation where mature TGFB1 signals within the confines of latent TGFB; the release and diffusion of TGFB1 is apparently not required. This “paracrine activation / autocrine signaling” model predicts that deletion of *Itgb8* on one cell type primarily affects another, and that deletion of *Tgfb1* will only affect the cells from which it is deleted. Here, we looked to test this model as it applies to microglial development.

To determine the developmental expression of *Tgfb1* in the brain, we examined published RNAseq atlases, which showed strong expression of *Tgfb1* in brain macrophages, and weaker expression in brain blood vessels (both endothelial cells and PDGFRβ+ mural cells) at E14.5 (Fig. 3A)[25]. Based on these data, we generated *Tgfb1* flox conditional mutants using a *Tgfb1* floxed exon 1 allele[26] and Cre lines to target macrophages/microglia (*Cx3cr1^{Cre}*), endothelial cells and macrophages/microglia (*Tie2^{Cre}*)[27], or vascular mural cells (pericytes and vascular smooth muscle cells) and fibroblasts (*Pdgfrb^{Cre}*)[28]. We compared vascular and microglia phenotypes in these conditional mutants to those in *Tgfb1$^{-/-}$* mice[29] which serve as a positive control (Fig. 3C).

As previously documented[29], *Tgfb1$^{-/-}$* mice showed prominent vascular changes (glomeruloid malformations, dilated and tortuous vessels) and associated hemorrhage throughout the cerebrum (“X” and asterisk in Fig. 3C). Concomitant with vasculopathy and hemorrhage, microglia in *Tgfb1$^{-/-}$* embryos completely lacked P2RY12 staining, even in microglia distant from hemorrhaging (Figure 3C). *Tgfb1$^{-/-}$* mutants therefore closely phenocopy *Itgb8$^{f/f}$;Nestin^{Cre}* mutants. *Tgfb1$^{f/f}$;Cx3cr1^{Cre}* mice displayed an identical microglia phenotype with loss of P2RY12 throughout the brain (Fig 3D). BAM cellular phenotypes were comparable to controls (not shown). *Tgfb1$^{f/f}$;Tie2^{Cre}* mice similarly had almost no P2RY12 expression, with the few P2RY12+ microglia lacking TdT-recombination reporter indicating lack of gene deletion in these cells (Figure 3E and data not shown). Interestingly,

Tgfb1$^{f/f}$*;Tie2*^{Cre} mutants had few vascular changes, although we did observe one or two sporadic, small hemorrhages in most embryos (Fig. 3 and data not shown). In contrast, while we also observed similar sporadic, small hemorrhages in most *Tgfb1*$^{f/f}$*;Pdgfrb*^{Cre} embryos, we did not see any change in P2RY12 expression (Fig. 3F), suggesting that hemorrhage and microglial phenotypes are separable. Taken together, these data indicate that embryonic microglial maturation requires self-produced TGFB1 and that TGFB1 expression in endothelial and mural cells (pericytes) cannot compensate for the maturational changes that result from *Tgfb1* deletion in microglia.

To determine the developmental stage at which *Tgfb1* signaling is important for microglial development, we re-examined bulk RNAseq from sorted microglia and BAMs[18] and observed that *Tgfb1* is highly expressed in both microglia and BAMs throughout development (Fig. 4A). In contrast, *P2ry12* and *Pf4* are specific markers for these cells and are expressed at early developmental stages. To conditionally delete *Tgfb1* from all macrophages in the developing brain, we generated *Tgfb1*$^{f/f}$*;Cx3cr1*^{CreER} and flox/null *Tgfb1*$^{fl/GFP}$*;Cx3cr1*^{CreER} E14.5 embryos from mothers treated with tamoxifen for three days after microglia have engrafted in the brain (E11.5-E13.5)[30,31]. *Tgfb1* RNAScope showed strong expression of *Tgfb1* in IB4+ blood vessels, IB4+ microglia and BAMs (meningeal and choroid plexus macrophages), and a loss of *Tgfb1* expression in microglia and macrophages in *Tgfb1*$^{f/f}$*;Cx3cr1*^{CreER} embryos (Fig. 4B,C). Similar to *Tgfb1*$^{f/f}$*;Cx3cr1*^{Cre} E14.5 embryos, we found that *Tgfb1*$^{f/f}$*;Cx3cr1*^{CreER} and *Tgfb1*$^{fl/GFP}$*;Cx3cr1*^{CreER} embryos had normal vasculature and no evidence of hemorrhage, but lacked microglial P2RY12 staining (Fig. 4C). To specifically delete *Tgfb1* in BAMs or microglia we relied on our previous findings that *Pf4*^{Cre} and *P2ry12*^{CreER} specifically drive recombination in these populations respectively[21]. After finding that *P2ry12*^{CreER} was unable to efficiently delete *Tgfb1* in all microglia, we sought to improve deletion efficiency by homozygosing *P2ry12*^{CreER}. We generated *Tgfb1*$^{fl/GFP}$*;P2ry12*$^{CreER/CreER}$*;Ai14* and *Tgfb1*$^{f/f}$*;P2ry12*$^{CreER/CreER}$*;Ai14* E14.5 embryos, inducing three days prior as with *Cx3cr1*^{CreER} mice. Importantly, *P2ry12*^{CreER} is a P2A fusion knock-in allele mice that retains P2RY12 protein expression in homo and heterozygous mice[21]. In contrast to *P2ry12-CreER* heterozygotes, which showed a partially penetrant phenotype, *Tgfb1*$^{fl/GFP}$*;P2ry12*$^{CreER/CreER}$*; Ai14* and *Tgfb1*$^{f/f}$*;P2ry12*$^{CreER/CreER}$*; Ai14* embryos had a complete loss of P2RY12 expression that was identical to embryos with *Cx3cr1*^{CreER}-mediated *Tgfb1* deletion (Fig. 4D). These data suggest that the microglial phenotype observed in these models is due to loss of *Tgfb1* in microglia, and not microglia progenitors or BAMs. To more directly test the function of *Tgfb1* in BAMs, we generated *Tgfb1*$^{f/f}$ *;Pf4*^{Cre}*; Ai14* E14.5 embryos. We previously showed that *Pf4*^{Cre} specifically recombines all BAMs including choroid plexus, meningeal and perivascular macrophages[21]. Consistent with this, we observed specific recombination of meningeal and choroid plexus macrophages in E14.5 control and *Tgfb1* conditional knockouts, but no changes in microglial P2RY12 expression (Figure 4E). Of note, *Pf4* is highly expressed in yolk sac myeloid precursors[32]. Retention of recombined tdT+ cells in border-associated spaces, and lack of recombination in microglia, indicate that *Pf4* is an early marker of BAM-committed cells. In total, our data indicate that *Tgfb1* is required well into mid-gestation for microglial development, provides additional evidence that vascular or BAM-expressed *Tgfb1* cannot compensate for the loss of *Tgfb1* in microglia, and suggests that that loss of *Tgfb1* in BAMs does not result in vascular or microglial dysfunction.

Tgfb1 is required to maintain postnatal microglial homeostasis

To assess whether there is an ongoing requirement for *Tgfb1* in microglial homeostasis we induced recombination in *Tgfb1*$^{f/f}$*;Cx3cr1*^{CreER} and *Tgfb1*$^{fl/GFP}$*;Cx3cr1*^{CreER} mice at P4,5,6. These mice were then collected at P30 for histological analysis. In *Tgfb1*$^{f/f}$*;Cx3cr1*^{CreER} and *Tgfb1*$^{fl/GFP}$*;Cx3cr1*^{CreER} mice given tamoxifen at P4,5,6, we found large patches of dysmature microglia – cells lacking expression of homeostatic markers (e.g. P2RY12), and with apparent upregulation of immature or reactive microglia markers. Among these patches were microglia that appeared similar to microglia in control mice. The size and distribution of patches was highly variable. Of note, *Tgfb*1 tamoxifen-inducible mutants exhibited no obvious neurobehavioral abnormalities, possibly due to sub-total and/or delayed acquisition of the dysmature microglia phenotype. To assay the degree of *Tgfb1* recombination in these mice, we performed RNAScope on *Tgfb1*$^{f/f}$*;Cx3cr1*^{CreER} mice, using probes targeting the floxed region of *Tgfb1*. This analysis showed that dysmature microglia lacked *Tgfb1*, while normal appearing microglia retained *Tgfb1* expression at levels similar to wild type mice (Fig. 4G) Remarkably, *Tgfb1*-expressing microglia and vascular cells were often found intermingled with *Tgfb1* cKO microglia indicating that *Tgfb1* from one cell cannot fully compensate for the loss of *Tgfb1* in neighboring cKO cells. Together these data further support the contention that *Tgfb1* is required cell autonomously to maintain neonatal microglial homeostasis.

Conditional Smad2/3 mutants reveal role for non-canonical TGFβ signaling in microglial homeostasis and neuromotor functioning.

After engaging the TGFβ-receptor, TGFβ signaling proceeds through both canonical (SMAD-dependent) and non-canonical (SMAD-independent) pathways (Fig 5A). To understand whether microglia abnormalities and associated neuromotor dysfunction can be attributed to canonical versus non-canonical TGFβ signaling, we generated *Smad2/3$^{f/f}$;Cx3cr1^{Cre}* mice and compared the behavioral, transcriptional and histological properties of these mice to *Tgfb1$^{f/f}$;Cx3cr1^{Cre}* mice[33,34]. Neither *Smad2/3$^{f/f}$;Cx3cr1^{Cre}* or *Tgfb1$^{f/f}$;Cx3cr1^{Cre}* mutants showed evidence of neonatal brain hemorrhage (data not shown). Following mice into adulthood, *Tgfb1$^{f/f}$;Cx3cr1^{Cre}* mice presented at 2 months of age with neuromotor dysfunction highly similar to 2-month-old *Itgb8$^{f/f}$;Nestin^{Cre}*, and *Tgfbr2$^{f/f}$;Cx3cr1^{Cre}* mice[7] and *Lrrc33$^{-/-}$* mice[5]. In contrast, *Smad2/3$^{f/f}$;Cx3cr1^{Cre}* mice showed no obvious behavioral abnormalities until 15 months of age, at which point some mice exhibited a slight tremor.

To understand why *Smad2/3* mutants lacked neurobehavioral symptoms comparable to other *Itgb8-Tgfb1* signaling mutants, we compared the transcriptional properties of *Itgb8*, *Lrrc33*, *Tgfb1*, *Tgfbr2* and *Smad2/3* conditional mutant models using whole brain and microglia bulk RNASeq (Figure 5B-E, Supplementary Figure 6). Whole brain transcriptomes from TGFβ pathway mutants were highly correlated, as would be expected from disrupting genes in a shared signaling pathway (Fig. 5B). Interestingly, *Lrrc33* and *Itgb8* mutants, the two most "proximal" to TGFB1 activation, were the two most highly correlated gene sets. In contrast, *Smad2/3* mutants, being the most distal from *Tgfb1* activation were the least correlated, possibly reflecting the accumulation of interceding non-canonical signaling pathways. We also identified several key differences among pathway mutants. First, we noticed that the pathway genes themselves were differentially altered in the various mutants (Fig. 5C) suggesting compensatory pathway feedback. Among these, *Lrrc33* is strongly upregulated in *Itgb8*, *Tgfb1*, and *Tgfbr2* mutants, compared to *Smad2/3* mutants in which *Lrrc33* is not differentially expressed. Beyond these potential feedback-associated gene changes, the most highly differentially expressed genes were largely microglia-specific, which we confirmed by comparing to bulk RNAseq of sorted microglia from each model Notably, the reduction in homeostatic and the increase in MGnD/DAM genes were generally less pronounced in *Smad2/3* mutants than in all other mutants, in association with the much less severe neuromotor phenotype (Fig. 5D and Supplemental Figure 5). We then reasoned that whole brain transcriptomic differences between *Smad2/3* mutants and other mutants could reveal gene sets relevant for neurobehavioral symptoms. Isolation of genes that were differentially expressed in *Tgfb1* and *Tgfbr2* mutants, but not *Smad2/3* mutants in isolated microglia and whole brain (Supplemental Figure 5) yielded several putative biological processes enriched in symptomatic mutants. Phagocytosis (vacuolar acidification), myelination, and synaptic pruning were among the most representative terms associated with *Tgfbr2$^{f/f}$;Cx3cr1^{Cre}* and *Tgfbr2$^{f/f}$;Cx3cr1^{Cre}* microglia and whole brain RNAseq gene sets, which also differentiate these models from *Smad2/3$^{f/f}$;Cx3cr1^{Cre}* mice (Supplemental Figure 5).

Among microglia-specific genes differentially expressed in *Smad2/3$^{f/f}$;Cx3cr1^{Cre}* versus other mutant models, we found *Apoe*, *Clec7a* and *Lgals3* to be particularly interesting (Fig. 5D). These genes are transiently enriched in populations of developmentally restricted microglia associated with myelin and axonal tracts (Axonal tract microglia, ATM), and in areas of active neurogenesis (proliferation associated microglia, PAM)[35]. Of note, we previously found evidence for delayed myelination in *Itgb8$^{f/f}$;Nestin^{Cre}* and *Tgfbr2$^{f/f}$;Cx3cr1^{Cre}* mutant mice[7].

Transcriptional changes in neuro-degenerative disease associated microglia (DAM or MGnD) depend on the APOE pathway, and MGnD signature genes, including *Spp1*, *Gpnmb,* and *Clec7a* are suppressed in disease models that also lack *Apoe*[36,37]. We were therefore interested to understand the degree to which *Apoe* might regulate PAM/MGnD signature genes, and whether increased expression of APOE in *Itgb8*, *Lrrc33*, *Tgfb1*, and *Tgfbr2* mutants might account for their more severe neuromotor symptoms. To that end, we generated *Tgfbr2$^{f/f}$;Cx3cr1^{Cre}; Apoe$^{+/-}$* and *Tgfbr2$^{f/f}$;Cx3cr1^{Cre}; Apoe$^{-/-}$* mutant mice, and evaluated their behavioral and neuroinflammatory (microglial) phenotypes at P90[38] (Supplemental Figure 6). Surprisingly, despite the transcriptomic similarity between dysmature and MGnD microglia, we found that deletion of APOE in *Tgfbr2$^{f/f}$;Cx3cr1^{Cre}* mice had no major effects on the neuromotor phenotype or microglial phenotypes (Supplemental Figure 6). This is similar to PAM/ATM microglia which also do not depend on APOE[35]. These data indicate that, unlike MGnD microglia, dysmature microglia do not depend on APOE for their polarization to occur, or alternatively, that non-canonical TGFβ signaling functions directly downstream of Apoe in microglial polarization.

We recently found that MGnD-polarized microglia can directly induce astrocyte activation similar to that observed in AD (in Review, Nature Immunology). Astrocyte activation is correlated with the degree of MGnD polarization, and is mechanistically linked to microglia expression of LGALS3. We sought to determine whether the differences in symptom severity in *Smad2/3$^{f/f}$;Cx3cr1^{Cre}* vs other pathway mutants can be attributed to relatively reduced expression of LGALS3, and whether SMAD2/3 mutant mice have evidence of correspondingly reduced astrocyte activation. To that end, we compiled a list of astrocyte activation markers from published data sets including models of brain injury and assessed the expression levels of these genes in our whole brain RNAseq dataset. This analysis revealed remarkable correlation among differentially expressed genes in *Itgb8*-TGFβ pathway mutants - *Itgb8*, *Lrrc33*,*Tgfb1*, and *Tgfbr2* pathway mutants, which have more polarized MGnD-like microglia compared to *Smad2/3$^{f/f}$;Cx3cr1^{Cre}* mice, also had more polarized astrocyte genes including *ApoE*, *GFAP*, *Fabp7*, and *Vimectin* (Fig. 5E). One potential mechanism for this differential polarization of astrocytes is the differential expression of *Lgals3*, a gene expressed by MgND microglia that we recently found to drive astrocyte polarization and neuropathology in a mouse model of Alzheimer's disease (in Review, Nature Immunology). Examination of LGALS3 expression by immunohistochemistry confirmed that LGALS3 expression was much higher in *Tgfb1$^{f/f}$;Cx3cr1^{Cre}* than *Smad2/3$^{f/f}$;Cx3cr1^{Cre}* mice, providing a potential explanation for the differential behavioral outcomes in these mice, despite the loss of microglial homeostatic markers in both models (Fig 5F-H). Interestingly, while most brain regions in *Smad2/3$^{f/f}$;Cx3cr1^{Cre}* mice did not show microglial LGALS3 expression, areas containing dense white matter, such as the corpus callosum, showed upregulation of LGALS3 (Fig 5H). *Tgfb1$^{f/f}$;Cx3cr1^{Cre}* also had much higher relative levels of microglial LGALS3 expression (arrowheads in Fig 5G) in the corpus callosum and fiber tracts of the striatum (arrowheads in 5G), suggesting that white matter microglia may be particularly reactive to the effects of TGFβ signaling disruption. Together, these data indicate that isolated disruption of canonical (SMAD-directed) TGFβ signaling in microglia results in neuropathologial phenotypes that are less severe than in mice with more proximal disruptions in the TGFβ signaling cascade, and that the disease-associated microglial gene LGALS3 may drive astrocytic changes seen in *Tgfb1$^{f/f}$;Cx3cr1Cre* mice that are less severe or absent in *Smad2/3$^{f/f}$;Cx3cr1^{Cre}* mice.

Discussion

Here, we show that that microglial differentiation is dependent upon the activation of microglial TGFB1 by *Itgb8*-expressing radial progenitors. Disruption of this signaling by conditionally deleting radial progenitor *Itgb8*, microglial *Tgfb1* or the downstream transcription factors *Smad2/3* in microglia results in a microglial transcriptional phenotype marked by the absence of mature microglial markers, persistent expression of genes normally expressed in microglial precursors, and heterogeneous accrual of reactive genes commonly found in transient developmental (PAM/ATM) or disease-associated (DAM/MGnD) microglia subsets. (Need to change this as we now see that MgND markers are expressed developmentally and are enriched in b8 mutants).

Interestingly, we find that domain-specific deletion of *Itgb8* in early embryonic radial progenitors results in microglial defects that are restricted to the brain regions created by these progenitors. Furthermore, consistent with recent reports that microglia are derived from a CD206+ precursor[19–21], and the earliest characterizations of microgliogenesis by del Rio-Hortega[22], we find that embryonic radial glial endfeet make direct contact with CD206+ meningeal macrophages. This is consistent with our model that the physical interaction between radial progenitors and immature microglia is crucial for radial glial *Itgb8*-mediated TGFβ signaling in microglia. This is also consistent with previous reports of microglial/radial glial interactions [39]. Lack of a similar microglial phenotype in *Itgb8$^{f/f}$;hGFAPCre* mutants, which recombine dorso-lateral radial progenitors ~3 and ~5 days after *Nestin^{Cre}* and *Emx1^{Cre}* respectively, places the timing of this interaction between E9 and E13.5, when microglia initially begin to invade the developing nervous system[40,13]. Remarkably, dysmature microglia in *Itgb8/Tgfb1* pathway mutants are highly similar to myeloid progenitors at this age. Our data are most consistent with recent fate-mapping data showing that microglia are derived from a CD206+ precursor and that disruption of *Itgb8/Tgfb1* signaling results in the maintenance of immature markers that would otherwise be downregulated, as well as the blockage of microglial marker expression. Future studies are needed to determine where and more precisely when this interaction occurs developmentally, and to better determine whether the specific interactions between ingressing microglia and radial glial basal and/or apical endfeet in the meninges or ventricular surface are necessary for microglial differentiation.

Our findings suggest that additional new models of brain region restricted microglial dysfunction can be created by deleting *Itgb8* in other radial progenitor domains. Taking advantage of the trans-activation of TGFB1 to create

genetic models of brain region-restricted microgliopathy is particularly useful, as microglial *Cre* and *CreER* lines generally recombine microglia throughout the nervous system, and not in particular brain regions[31,41,42,43]. We believe that the study of brain region-restricted microglial dysfunction will provide crucial information about how microglial dysfunction in particular brain regions contributes in a modular fashion to more complex behavioral and cognitive disruptions seen in other animal models and in humans with pervasive neurodevelopmental immune dysfunction. Combining mouse models of neuroinflammatory or neurodegenerative disease with brain region-specific *Itgb8* conditional knock-out models will be especially illuminating.

In line with recent cryoEM data[10,11], we show that microglia depend on cell-autonomous expression of *Tgfb1* for their early maturation. Interestingly, we only observe a fulminant vascular/hemorrhage phenotype in *Tgfb1* null mice; deletion of *Tgfb1* in endothelial cells and microglia ($Tie2^{Cre}$), or in vascular mural cells and fibroblasts ($Pdgfrb^{Cre}$) had no major effect on cerebrovascular morphogenesis or barrier function. Therefore, vessel-expressed TGFB1 is apparently dispensible for microglial maturation, but the source of *Tgfb1* for vascular maturation remains unknown. Fitting with the paracrine activation / autocrine signaling model, we propose radial glia ITGB8 activates TGFB1 on endothelial cells and/or pericytes, so that the loss of endothelial *Tgfb1* can be compensated by pericyte TGFB1 or vice versa. It is also possible that TGFB1 in the embryonic circulation can compensate for the loss of vascular TGFB1[29].

In contrast to *Itgb8* which we show is largely dispensable for maintaining microglial homeostasis, we find that microglial *Tgfb1* is necessary for microglial homeostasis postnatally. One potential explanation for this discrepancy could be the activation of TGFB1 by other integrin complexes or by integrin-independent pathways postnatally. The apparent absence of phenotype in mice with disruption of *Itgb8* after birth is particularly important in considering *Itgb8*-targeting therapeutics. We recently found that antibody-based blockade of ITGB8 in AD mouse models enhances MGnD polarization and reduces the size of amyloid plaques (in Review, Nature Immunology). Altogether, our studies present a model for microglial development whereby interactions between neural progenitor and immature microglia are necessary for the avb8-dependent activation of microglial TGFB1.

Acknowledgements

This study was in supported in part by HDFCC Laboratory for Cell Analysis Shared Resource Facility through a grant from NIH (P30CA82103). This research was supported, in part, by the UCSF Vision Core shared resource of the NIH/NEI P30 EY002162. We would like to thank Marie La Russa for helpful manuscript editing suggestions. We would like to thank Dr. Richard Flavell for providing $Cx3cr1^{Cre}$ and $Cx3cr1^{GFP}$ mice. We would also like to thank Dr. Rosemary Ackhurst for providing *Tgfb1* null mice.

Author Contributions

T.A. supervised the study, performed the behavioral analysis in Figure S1 and did the cell counting in Figure S2. G.L.M. designed the study, under the supervision of T.A. G.L.M. performed the histological analysis, with specific contributions from others listed here. N.S. performed preliminary histological analysis of postnatal $Tgfb1^{F/F}/Tgfb1^{F/GFP}$; $Cx3cr1^{Cre}$ and $Smad2/3^{f/f}$; $Cx3cr1^{Cre}$ mice. G.L.M performed the imaging, with support from T.A. for Figure S2. Mouse husbandry was done by G.L.M., with support from N.S., who initially bred $Tgfb1^{F/F}/Tgfb1^{F/GFP}$; $Cx3cr1^{Cre}$ and $Smad2/3^{f/f}$; $Cx3cr1^{Cre}$ mice, and with support from A.K., L.T., M.B., K.C, and D.M.. G.L.M. performed RNA isolation and bulk RNA-seq experiments for Figure 7. N.S. performed bioinformatic analysis in Fig. 2 and 7. X.Z. performed RNA-seq analysis of sorted microglia in $Itgb8^{f/f}$;$Emx1^{Cre}$ mice for Figure 2, with bioinformatic support from K.K. A.K and L.T sectioned *Tie2-Cre* and *PdgfRb-Cre* embryos used in Fig 3. G.L.M. performed the flow cytometry experiments to isolate microglia from $Tgfb1^{F/F}$; $Cx3cr1^{Cre}$ mice, with support from C.O. C.O. performed the flow cytometry experiments to isolate microglia from $Smad2/3^{f/f}$; $Cx3cr1^{Cre}$ mice. L.T. collected and stained embryos used in the *Emx1-Cre; RG-Brainbow* analysis. H.K. helped to collect $Nestin^{Cre}$ embryos used in Fig 1. H.P. provided the *Itgb8-TdT* mouse line and E.S. provided *RG-Brainbow* mouse line. K.A. supervised C.O. D.S. provided input regarding experimental design and interpretation. O.B. supervised work by X.Z. and K.K. The manuscript was written by G.L.M and T.A..

Competing Interests

D.S. and UCSF hold patents on the uses of antibodies that block the alphavbeta8 integrin. D.S. is a founder and owns stock in Pliant Therapeutics, is on the Scientific Review Board for Genentech and is on the Inflammation Scientific Review Board for Amgen.

Figure Legends

Figure 1. Deletion of *Itgb8* in early embryonic radial glia disrupts microglial maturation.
A) Analysis of *Itgb8* expression in the E14.5 mouse embryo in neural progenitor cells (NPCs) and radial glia, microglia, endothelial cells, and mural cells[44]. **B)** *Itgb8-TdT* reporter expression confirms strong *Itgb8* expression in SOX9+NESTIN+ radial progenitors at E14.5. Open arrowhead marks radial glia fibers; closed arrowhead marks ramified radial glia endfeet at the surface of the neuroepithelium. **C)** Model describing developmental expression of *Itgb8* in neuroepithelium and radial glia, and correlation with sequential timing of Cre recombination in *Emx1^{Cre}*, *Nestin^{Cre}* and *hGFAP^{Cre}* lines. (see also Supplementary Figures 2 and 3). **D-F)** Deletion of *Itgb8* from neuroepithelial and radial progenitors using indicated Cre lines**.** Coronal brain sections stained for tdT (Cre recombination, red), vascular endothelium (CD31, cyan), and macrophages/microglia (IBA1, yellow); hemorrhage (red blood cells marked by TER119 (yellow) observed outside of vascular lumen (CD31, cyan) and microglia precursors (CD206, yellow) and committed/homeostatic microglia (P2RY12, cyan). G**)** E14.5 brain section from *Emx1^{Cre};RG-brainbow* mouse stained for membranous GFP (individual recombined radial glia; endfeet, green), microglia precursors (CD206, magenta), and committed/homeostatic microglia (P2RY12, yellow). Arrowheads indicate foot process of radial glia contacting presumptive pial-associated CD206+ microglia precursor (model to right). Scale bar in B=500μm, D=200μm, G=25 μm.

Figure 2. *Emx1-Cre* deletion of *Itgb8* results in anatomically restricted blockage of microglial differentiation.
A) Comparison of the transcriptional properties of adult *Itgb8$^{f/f}$; Emx1^{Cre}* mutant and control microglia to stage specfic developmental markers reveals that dysmature microglia retain the gene expression profiles of early embryonic microglia.[24] **B)** Analysis of developmental gene cluster expression reveals enrichment for progenitor (cluster 1) and early embryonic phase (clusters 3-5) enriched gene sets. **C)** Whole brain sagittal immunostaining of adult *Itgb8$^{f/f}$; Emx1^{Cre}* mice revealed anatomically restricted maintenance of the microglial precursor marker CD206 in the cortex and hippocampus (asterisk), accompained by loss of the homeostatic marker P2RY12. **D)** Increased expression of the MGnD marker LGALS3 in a subset of cortical and hippocampal microglia in *Itgb8$^{f/f}$; Emx1^{Cre}* mice (asterisk). Closed and open arrowheads in **E-G)** mark cortical and striatal microglia respectively. **E)** Downregulation of the microglial homeostatic marker TMEM119 in the cortex of a *Itgb8$^{f/f}$; Emx1^{Cre}* mouse. **F)** Cortex-restricted upregulation of the microglial reactive marker APOE in IBA1+ cells of the cortex (green cells). **D)** Cortex-restricted upregulation of the microglial reactive marker CLEC7a. Cx= cerebral cortex; Cc= corpus callosum; Str= striatum; Dashed line= cortical/striatal boundary. Scale bar in C= 2mm, E=150μm.

Figure 3. Microglial dysmaturation due to *Tgfb1* deletion in microglia/macrophages.
A) Analysis of the embryonic expression of *Tgfb1* in E14.5 neural progenitors, microglia, endothelial and mural cells (from [44]) **B,C)** E14.5 coronal brain sections from control (*Tgfb$^{+/-}$*) embryos, or embryos with global (*Tgfb1$^{-/-}$*) or cell-lineage specific deletion of *Tgfb1* (*Tgfb1$^{fl/fl}$*) in **D)** macrophages/microglia (*Cx3cr1^{Cre}*), **E)** endothelial cells and microglia/macrophages (*Tie2^{Cre}*), or **F)** vascular mural cells (*Pdgfbrb^{Cre}*) were stained for hemorrhage (TER119, magenta) and vasculature (CD31, green); microglia/macrophage (IBA1, magenta) association with blood vessels (CD31, green); and committed/hemostatic microglia (P2RY12, magenta). Only *Tgfb1$^{-/-}$* mutants have consistent evidence of vascular dysplasia (marked by X) and hemorrhage (asterisk), whereas mice with microglia/macrophage deletion of *Tgfb1* (*Tgfb$^{-/-}$*, *Tgfb1$^{fl/fl}$;Cx3cr1^{Cre}* and *Tgfb1$^{fl/fl}$;Tie2Cre* mutants) have presence of dysmature microglia (open arrowheads, blowups to right). Scale bar in B=150μm.

Figure 4. Microglia provide their own TGFB1 to promote and maintain homeostasis.
A) Sorted bulk-Seq analysis[18] of embryonic microglia and BAMs reveals that *Tgfb1* is expressed in both microglia and BAMs during embryonic develpoment, whereas *P2ry12* and *Pf4* are specific markers of these two respective

populations. **B,C)** Analysis of control **(B)** and conditional *Cx3cr1*^{CreER} mediated deletion of *Tgfb1* deletion in the E14.5 forebrain following E11.5, 12.5 and 13.5 tamoxifen induction. Analysis revealed no hemorrhage (CD31 in green, TER119 in magenta), no change in macrophage/blood vessel association (IBA1 in magenta, CD31 in green), loss of the homeostatic marker P2RY12 (in magenta, IBA1 in green), and loss of *Tgfb1* (cyan) in Isolectin B4 (green) and Tdt (red) labeled microglia, but not in IB4 + labeled blood vessels. **D)** Analysis of conditional *P2ry12*^{CreER} mediated deletion of *Tgfb1* deletion in E14.5 microglia the following E11.5, 12.5 and 13.5 tamoxifen induction. Analysis revealed no brain hemorrhage (CD31 in green, TER119 in magenta), no change in macrophage/blood vessel association (IBA1 in magenta, CD31 in green), and loss of the homeostatic marker P2RY12 (magenta), in IBA1+ (green) microglia. **E)** Analysis of conditional *Pf4*^{Cre} mediated deletion of *Tgfb1* deletion in the E14.5 forebrain. Analysis revealed no brain hemorrhage (CD31 in green, TER119 in magenta), no change in macrophage/blood vessel association (IBA1 in magenta, CD31 in green), and no loss of the homeostatic marker P2RY12 (magenta), in IBA1+ (green) microglia. **F)** Bulk-seq analysis of *Tgfb1* expression in the adult mouse brain[25]. Analysis revealed enrichment for *Tgfb1* expression primarily in microglia and vascular cells. **G)** Analysis of conditional *Cx3cr1*^{CreER} mediated deletion of *Tgfb1* deletion in the P30 mouse brain following neonatal tamoxifen induciton at P4,5 and 6. Analysis revealed a "patchy" distribution of *Tgfb1* negative microglia with altered morphology and loss of P2RY12 (open arrowheads in 1) adjacent to patches of microglia with no loss of *Tgfb1* or P2RY12. Scale bar in B=150μm, G=100μm.

Figure 5. Disruption of non-canonical TGFβ signaling in microglia drives disease-associated gene expression.
A) Schematic of TGFβ, with mutant mouse models analyzed by bulk and microglial flow cytometry noted by color (*Itgb8*=red; *Tgfb1*=cyan; *Lrrc33*=orange; *Tgfb2*=blue, *Smad2/3*=green). **B)** Correlation of bulk-seq gene expression across TGFβ mutant models. **C)** Compensatory transcriptional changes of key TGFβ signaling genes in different TGFβ mutant models. **D)** Bulk-seq analysis of microglial homeostatic and disease associated (MgND/DAM) microglial markers across TGFβ mutant models. **E)** Bulk-seq analysis of astrocytosis-associated markers across TGFβ mutant models. **F-G)** Comparison of control **(F)** *Tgfb1*$^{fl+/}$*;Cx3cr1*^{Cre}*,* **(G)** *Tgfb1*$^{fl/fl}$*;Cx3cr1*^{Cre} *and* **(H)** *Smad2/3*$^{f/f}$*;Cx3cr1*^{Cre} adult mice. Analysis revealed loss of the homeostatic marker P2RY12 in both conditional *Tgfb1* and *Smad2/3* mutants, but significantly higher upregulation of the MGnD-associated microglial marker LGALS3 (see arrowheads). LGALS3 upregulation in *Tgfb1* conditional mutants was significantly higher in white matter (asterisk in **G and H**) and was only seen in the white matter of *Smad2/3* conditional mutants (**H**). Scale bar in F=50μm.

Methods:

Key Resources Table:

Reagent type	Designation	Source of references	Identifiers	Additional information
Mouse line	*Ai14*	JAX	Stock No: 007914. RRID:IMSR_JAX:007914.	
Mouse line	*Aldh1L1-CreER*	JAX	Stock No: 029655. RRID:IMSR_JAX:029655.	
Mouse line	*ApoE null*	JAX	Stock No: :002052. RRID:IMSR_JAX::002052.	
Mouse line	*CAG-Sun1/sfGFP*	JAX	Stock# 030952. RRID: IMSR_JAX:030952.	
Mouse line	*Cx3cr1-Cre*	JAX	Stock No: 025524. RRID:IMSR_JAX:025524.	
Mouse line	*Cx3cr1-CreER*	JAX	Stock No: 020940. RRID:IMSR_JAX:020940.	
Mouse line	*Emx1-IRES-Cre*	JAX	Stock No: 005628. RRID:IMSR_JAX:005628	
Mouse line	*hGFAP-Cre*	JAX	Stock No: 004600. RRID:IMSR_JAX:004600.	
Mouse line	*iSure-Cre*	(Fernández-Chacón et al. 2019)	MGI:6361145.	
Mouse line	*Itgb8 flox*	(Proctor et al. 2005)	MGI: 3608910.	
Mouse line	*Itgb8-tdT*	(Nakawesi et. al. 2021)	Obtained from Dr. Helena Paidassi.	
Mouse line	*Nestin-Cre*	JAX	Stock No: 003771. RRID:IMSR_JAX:003771.	
Mouse line	*Olig2-Cre*	JAX	Stock No:025567. RRID:IMSR_JAX:025567.	

Mouse line	*P2ry12-CreER*	JAX	Stock No: 034727. RRID:IMSR_JAX:034727.	
Mouse line	*PdgfRb-Cre*	JAX	MGI:6361145.	
Mouse line	*Pf4-Cre*	JAX	Stock No: 008535. RRID:IMSR_JAX:008535.	
Mouse line	*RG-Brainbow*	(Nakagawa et. al. 2019)	Obtained from Dr. E. S. Anton.	
Mouse line	*Smad2 flox*	JAX	Stock No: 022074. RRID:IMSR_JAX:022074	
Mouse line	*Smad3 flox*	JAX	MGI: 3822465.	
Mouse line	*Syn1-Cre*	JAX	Stock No: 003966. RRID:IMSR_JAX:003966.	
Mouse line	*Tgfb1 flox*	JAX	Stock No: RRID:IMSR_JAX:	
Mouse line	*Tgfb1 null*	(Kulkarni et. al. 1993)	MGI: 1857671.	
Mouse line	*Tgfb1-GFP*	(Li et. al. 2007)	MGI: 3719583	
Mouse line	*TgfbR2 flox*	(Chytil et. al. 2002)	MGI: 2384513.	
Mouse line	*Tie2-Cre*	JAX	Stock No: 008863. RRID:IMSR_JAX:008863.	
Mouse line	*Ubc-CreER*	JAX	Stock No: 007001. RRID:IMSR_JAX:007001.	
Antibody	ApoE	Abcam	Rabbit monoclonal. Cat# ab183596. RRID:AB_2832971.	Used at 1:300.
Antibody	CD206	Biorad	Rat monoclonal antibody. Cat#: MCA2235T. RRID:AB_1101333.	Used at 1:150.
Antibody	CD11b-PE-Cy7	eBioscience	Rat monoclonal antibody. Cat#: 50-154-54. RRID: AB_469588.	
Antibody	CD31	R&D Systems	Goat polyclonal antibody. Cat# AF3628; RRID: AB_2161028	Used at 1:300.
Antibody	Clec7a	BioLegend	Rat monoclonal antibody. Cat#: 144302: RRID:AB_2561519	Used at 1:300.
Antibody	Fcrls-APC	Butovsky lab	Rat monoclonal antibody. Clone 4G11.	
Antibody	EGFP	Origene	Goat polylonal antibody. Cat#: R1091P. RRID:AB_1002036.	Used at 1:2000.
Antibody	IB4-488	Thermo Fisher	Cat#: I21411. RRID:AB_2314662.	Used at 1:150.
Antibody	IBA1	Novus	Goat polyclonal antibody. Cat#:NB100-1028. RRID:AB_521594.	Used at 1:300.
Antibody	IBA1	Wako	Rabbit polyclonal antibody. Cat#: 019-19741; RRID: AB_839504	Used at 1:300.
Antibody	LGALS3	CedarLane	Rat monoclonal antibody. Cat#:CL8942AP. RRID:AB_10060357.	Used at 1:150.
Antibody	Ly-6C-PerCP/Cy5.5	Biolegend	Rat monoclonal antibody. Cat#: 128012. RRID:AB_1659241.	
Antibody	Nestin-488	Abcam	Mouse monoclonal antibody. Cat#: ab197495. RRID:AB_2732861.	Used at 1:150.
Antibody	NeuN	Millipore	Mouse monoclonal antibody. Cat#: MAB377. RRID:AB_2298772.	Used at 1:100.
Antibody	Olig2-Rb	Millipore	Rabbit polyclonal antibody. Cat#:: AB9610. RRID:AB_570666.	Used at 1:300.
Antibody	P2ry12	Anaspec	Rabbit polyclonal antibody. Cat# 55043A. RRID:AB_2298886.	Used at 1:500.
Antibody	P2ry12	A generous gift from Dr. David Julius.	Rabbit polyclonal antibody.	Used at 1:1000.
Antibody	PdgfRa	R & D Systems	Goat polyclonal antibody. Cat#AF1062. RRID:AB_2236897.	Used at 1:300.
Antibody	GFAP	DAKO	Rabbit polyclonal antibody. Cat#Z0334.RRID:AB_10013382.	Used at 1:300.
Antibody	pSmad3 (S423/S425)	Abcam	Rabbit monoclonal antibody. Cat# ab52903; RRID: AB_882596	Used at 1:100.
Antibody	Sox9	R and D Systems	Goat polyclonal antibody. Cat#: AF3075. RRID:AB_2194160.	Used at 1:300.
Antibody	Ter119	R&D Systems	Rat polyclonal antibody. Cat# MAB1125; RRID: AB_2297123.	Used at 1:150.

Antibody	Tmem119	Abcam	Rabbit monoclonal antibody. Cat#: ab209064. RRID:AB_2800343.	Used at 1:100.
Molecular Biology Reagent	Opal secondaries	Okaya Biosciences	Cat#:FP1488001KT.	Used at 1:750
Molecular Biology Reagent	RNAscope Multiplex Fluorescent Reagent Kit v2	ACD Biosciences	Cat #323100.	
Molecular Biology Reagent	Percoll Plus	GE Healthcare	Cat#17-5445-02	

Mice: All mouse work was performed in accordance with UCSF Institutional Animal Care and Use Committee protocols. Please see key resources table for additional mouse line information.

Histology and Immunostaining: Adult mouse mouse brains were harvested at P60-P90 following transcardial perfusion with 20 mL cold PBS and 20 mL cold 4% formaldehyde. Brains and embryos were fixed overnight at 4 degrees in 4% formaldehyde, followed by overnight incubation in 30% sucrose. Samples were embedded (Tissue Plus O.C.T. Compound, Fisher Scientific) and sectioned at 20 µm. Some adult brains were sectioned at 40um. Sections were immunostained using a blocking/permeabilization buffer of PBS containing 2% BSA, 5% donkey serum and. 5% TritonX-100. Primary and secondary antibodies were diluted in PBS containing 1% BSA and. 25% TritonX-100. Secondary antibodies conjugated to Alexa fluorophores were used at 1:300 (Jackson ImmunoResearch). Immunostained sections were mounted with Prolong Gold Antifade Mountant (Thermofisher P36930). Please see Key Resources Table for list of antibodies and the relevant concentrations used for immunofluorescence.

RNAscope: 20um cryosectioned tissue sections were processed for RNAscope using the manufactures protocol for cryosectioned tissue and reagents from the RNAscope Multiplex Fluorescent Reagent Kit v2 (Cat #323100) and Opal secondaries (Okaya Biosciences FP1488001KT). A custom RNAscope probe set was used to target the floxed exon 1 of *Tgfb1* (Cat #1207831-C1). Slides were hybridized in the ACD HybEZ II Oven (Cat #321711).

Tamoxifen induction: Recombination was induced by three doses of tamoxifen dissolved in corn oil, administered by oral gavage every other day (150 µL of 20 mg/mL). For embryonic mouse inductions, pregnant dams were given tamoxifen (150 µL of 20 mg/mL) on E13.5, E15.5 and E17.5, for a total of three gavage injections. Neonatal tamoxifen injections were done at P4,5, and 6, at a dosage of 500μg injected intraperitonealy (50uL of a 10mg/mL solution in corn oil). All mouse work was performed in accordance with UCSF Institutional Animal Care and Use Committee protocols. Mice had food and water ad libitum. The *P2ry12-CreER* mouse line will be deposited at Jackson Labs (Stock #034727) and at the Mutant Mouse Resource and Research Center (MMMRC).

Flow cytometry: The *Itgb8*$^{fl/fl}$*;Emx1*^{Cre} Mice were euthanized in a CO_2 chamber and then transcardially perfused with 10 ml cold Hanks' Balanced Salt Solution (HBSS, ThermoFisher, 14175103). The mouse brain was isolated and the cortex was dissected from one hemisphere for microglia purification using the standardard isolation procedure established in Butovsky lab[45] Briefly, the cortex was homogenized and resuspended with 5 ml 70% Percoll Plus (GE Healthcare, 17-5445-02) and 5 ml 37% Percoll Plus placed on top. The microglia were enriched in the interface layer after centrifugation in 800 g, 4°C, for 25 min with an acceleration of 2 and a deceleration of 1. The microglia enriched cell population were stained with PE-Cy7 anti-mouse CD11b (1:300, eBioscience, 50-154-54), APC anti-mouse Fcrls (1:1000, clone 4G11, Butovsky Lab), and PerCP/Cy5.5 anti-mouse Ly-6C (1:300, Biolegend, 128012). The cells were then processed by a BD FACSAria™ II (BD Bioscience) and CD11b^{+}Fcrls^{+} Ly-6C^{-} cells were sorted into Eppendorf tubes for RNA-seq. Microglia from *Smad2/3*$^{f/f}$*;Cx3cr1*^{Cre} and *Tgfb1*$^{f/f}$*;Cx3cr1*^{Cre} mice were isolated as previously described by the Arnold lab[42].

Imaging: Confocal images were taken with 10x, 20x or 40x objectives using a motorized Zeiss 780 upright laser scanning confocal microscope or a motorized Zeiss 900 inverted laser scanning confocal microscope. Image brightness and contrast was optimized in ImageJ. Images and figures were arranged in Adobe Illustrator.

Statistical analysis: Sample size was not precalculated using a statistical framework, but conformed to general standards in the field. Sample analysis was not blinded. For all immunostaining quantification, values for each mouse were calculated by averaging three pictures from each mouse. Differences between means were compared using a two-tailed t-test, with an alpha of 0.05.

RNA sequencing:
For the sequencing of microglia isolated from *Itgb8*$^{f/f}$ *;Emx1*^{Cre} mice, one thousand sorted microglia resuspended in 5 ml TCL buffer with 1% 2-Mercaptoethanol were placed into a 96-well plate and sent to Broad Technology Labs for Smart-Seq2 following their standard protocol. Briefly, cDNA libraries were generated using the Smart-seq2 protocol[46]. The amplified and barcoded cDNA libraries were loaded into Illumina NextSeq500 sequencer using a High Output v2 kit to generate 2 × 25 bp reads. For whole brain samples, RNA isolation was performed using dounce homogenization and Trizol extraction and alcohol precipitation. For Total RNA from FACS-sorted microglia from *Smad2/3*$^{f/f}$*;Cx3cr1*^{Cre} and *Tgfb1*$^{f/f}$*;Cx3cr1*^{Cre} mice, RNA was isolated using the QIAGEN RNAeasy micro kit. PolyA+ unstranded libraries were synthesized from total RNA (RIN > 6) with NEBNext Ultra II RNA Library Prep Kit and sequenced in a Illumina HiSeq4000 system (150 pb paired-end setting). Demultiplexed fastq files were aligned to the mouse genome (mm10) with Rsubread and quantified with FeatureCounts. Count normalization and differential expression analysis were performed with DESeq2. Correlations between multiple datasets were computed with the cor() function from base R and visualized using the corrplot package. Heatmaps were generated with the pheatmap package. Venn diagrams were produced with standard GNU coreutils and drawn in Inkscape. Overrepresentation analysis was performed using PANTHER from the GO portal. Datasets used in this study are as follows: newly generated data (whole brain data, isolated Tgfb1 mutant microglia data) have been deposited into the GEO database and will be made public upon publication. *Itgb8*$^{f/f}$*;Emx1*^{Cre} microglia and *Smad2/3*$^{f/f}$*;Cx3cr1*^{Cre} data were retrieved from the GEO database and will also be made public upon publication. *Tgfbr2*$^{F/F}$*;Cx3cr1*^{Cre} microglia is from GEO GSE124868. Data from *Lrrc33-/-* microglia and whole brain was obtained from GEO GSE96938.

References

1. Spittau, B., Dokalis, N., and Prinz, M. (2020). The Role of TGFβ Signaling in Microglia Maturation and Activation. Trends in Immunology *41*, 836–848. 10.1016/j.it.2020.07.003.

2. Bohlen, C.J., Bennett, F.C., Tucker, A.F., Collins, H.Y., Mulinyawe, S.B., and Barres, B.A. (2017). Diverse Requirements for Microglial Survival, Specification, and Function Revealed by Defined-Medium Cultures. Neuron *94*, 759-773.e8. 10.1016/j.neuron.2017.04.043.

3. Butovsky, O., Jedrychowski, M.P., Moore, C.S., Cialic, R., Lanser, A.J., Gabriely, G., Koeglsperger, T., Dake, B., Wu, P.M., Doykan, C.E., et al. (2014). Identification of a unique TGF-β–dependent molecular and functional signature in microglia. Nat Neurosci *17*, 131–143. 10.1038/nn.3599.

4. Brionne, T.C., Tesseur, I., Masliah, E., and Wyss-Coray, T. (2003). Loss of TGF-β1 Leads to Increased Neuronal Cell Death and Microgliosis in Mouse Brain. Neuron *40*, 1133–1145. 10.1016/S0896-6273(03)00766-9.

5. Wong, K., Noubade, R., Manzanillo, P., Ota, N., Foreman, O., Hackney, J.A., Friedman, B.A., Pappu, R., Scearce-Levie, K., and Ouyang, W. (2017). Mice deficient in NRROS show abnormal microglial development and neurological disorders. Nat Immunol *18*, 633–641. 10.1038/ni.3743.

6. Qin, Y., Garrison, B.S., Ma, W., Wang, R., Jiang, A., Li, J., Mistry, M., Bronson, R.T., Santoro, D., Franco, C., et al. (2018). A Milieu Molecule for TGF-β Required for Microglia Function in the Nervous System. Cell *174*, 156-171.e16. 10.1016/j.cell.2018.05.027.

7. Arnold, T.D., Lizama, C.O., Cautivo, K.M., Santander, N., Lin, L., Qiu, H., Huang, E.J., Liu, C., Mukouyama, Y., Reichardt, L.F., et al. (2019). Impaired αVβ8 and TGFβ signaling lead to microglial dysmaturation and neuromotor dysfunction. Journal of Experimental Medicine *216*, 900–915. 10.1084/jem.20181290.

8. Buttgereit, A., Lelios, I., Yu, X., Vrohlings, M., Krakoski, N.R., Gautier, E.L., Nishinakamura, R., Becher, B., and Greter, M. (2016). Sall1 is a transcriptional regulator defining microglia identity and function. Nature Immunology *17*, 1397–1408. 10.1038/ni.3585.

9. Zöller, T., Schneider, A., Kleimeyer, C., Masuda, T., Potru, P.S., Pfeifer, D., Blank, T., Prinz, M., and Spittau, B. (2018). Silencing of TGFβ signalling in microglia results in impaired homeostasis. Nat Commun *9*, 4011. 10.1038/s41467-018-06224-y.

10. Campbell, M.G., Cormier, A., Ito, S., Seed, R.I., Bondesson, A.J., Lou, J., Marks, J.D., Baron, J.L., Cheng, Y., and Nishimura, S.L. (2020). Cryo-EM Reveals Integrin-Mediated TGF-β Activation without Release from Latent TGF-β. Cell *180*, 490-501.e16. 10.1016/j.cell.2019.12.030.

11. Duan, Z., Lin, X., Wang, L., Zhen, Q., Jiang, Y., Chen, C., Yang, J., Lee, C.-H., Qin, Y., Li, Y., et al. (2022). Specificity of TGF-β1 signal designated by LRRC33 and integrin αVβ8. Nat Commun *13*, 4988. 10.1038/s41467-022-32655-9.

12. Tronche, F., Kellendonk, C., Kretz, O., Gass, P., Anlag, K., Orban, P.C., Bock, R., Klein, R., and Schütz, G. (1999). Disruption of the glucocorticoid receptor gene in the nervous system results in reduced anxiety. Nat Genet *23*, 99–103. 10.1038/12703.

13. Anthony, T.E., and Heintz, N. (2008). Genetic lineage tracing defines distinct neurogenic and gliogenic stages of ventral telencephalic radial glial development. Neural Development *3*, 30. 10.1186/1749-8104-3-30.

14. Graus-Porta, D., Blaess, S., Senften, M., Littlewood-Evans, A., Damsky, C., Huang, Z., and Orban, P. ᴺ1-Class Integrins Regulate the.

15. Loo, L., Simon, J.M., Xing, L., McCoy, E.S., Niehaus, J.K., Guo, J., Anton, E.S., and Zylka, M.J. (2019). Single-cell transcriptomic analysis of mouse neocortical development. Nat Commun *10*, 134. 10.1038/s41467-018-08079-9.

16. Nakawesi, J., This, S., Hütter, J., Boucard-Jourdin, M., Barateau, V., Muleta, K.G., Gooday, L.J., Thomsen, K.F., López, A.G., Ulmert, I., et al. (2021). αvβ8 integrin-expression by BATF3-dependent dendritic cells facilitates early IgA responses to Rotavirus. Mucosal Immunology *14*, 53–67. 10.1038/s41385-020-0276-8.

17. Gorski, J.A., Talley, T., Qiu, M., Puelles, L., Rubenstein, J.L.R., and Jones, K.R. (2002). Cortical Excitatory Neurons and Glia, But Not GABAergic Neurons, Are Produced in the Emx1-Expressing Lineage. J. Neurosci. *22*, 6309–6314. 10.1523/JNEUROSCI.22-15-06309.2002.

18. Utz, S.G., See, P., Mildenberger, W., Thion, M.S., Silvin, A., Lutz, M., Ingelfinger, F., Rayan, N.A., Lelios, I., Buttgereit, A., et al. (2020). Early Fate Defines Microglia and Non-parenchymal Brain Macrophage Development. Cell *181*, 557-573.e18. 10.1016/j.cell.2020.03.021.

19. Hattori, Y., Kato, D., Murayama, F., Koike, S., Asai, H., Yamasaki, A., Naito, Y., Kawaguchi, A., Konishi, H., Prinz, M., et al. (2023). CD206+ macrophages transventricularly infiltrate the early embryonic cerebral wall to differentiate into microglia. Cell Reports *42*, 112092. 10.1016/j.celrep.2023.112092.

20. Masuda, T., Amann, L., Monaco, G., Sankowski, R., Staszewski, O., Krueger, M., Del Gaudio, F., He, L., Paterson, N., Nent, E., et al. (2022). Specification of CNS macrophage subsets occurs postnatally in defined niches. Nature *604*, 740–748. 10.1038/s41586-022-04596-2.

21. McKinsey, G.L., Lizama, C.O., Keown-Lang, A.E., Niu, A., Santander, N., Larpthaveesarp, A., Chee, E., Gonzalez, F.F., and Arnold, T.D. (2020). A new genetic strategy for targeting microglia in development and disease. eLife *9*, e54590. 10.7554/eLife.54590.

22. Rio-Hortega, P. (1939). THE MICROGLIA. The Lancet *233*, 1023–1026. 10.1016/S0140-6736(00)60571-8.

23. Nakagawa, N., Plestant, C., Yabuno-Nakagawa, K., Li, J., Lee, J., Huang, C.-W., Lee, A., Krupa, O., Adhikari, A., Thompson, S., et al. (2019). Memo1-Mediated Tiling of Radial Glial Cells Facilitates Cerebral Cortical Development. Neuron *103*, 836-852.e5. 10.1016/j.neuron.2019.05.049.

24. Thion, M.S., Low, D., Silvin, A., Chen, J., Grisel, P., Schulte-Schrepping, J., Blecher, R., Ulas, T., Squarzoni, P., Hoeffel, G., et al. (2018). Microbiome Influences Prenatal and Adult Microglia in a Sex-Specific Manner. Cell *172*, 500-516.e16. 10.1016/j.cell.2017.11.042.

25. Zhang, Y., Chen, K., Sloan, S.A., Bennett, M.L., Scholze, A.R., O'Keeffe, S., Phatnani, H.P., Guarnieri, P., Caneda, C., Ruderisch, N., et al. (2014). An RNA-Sequencing Transcriptome and Splicing Database of Glia, Neurons, and Vascular Cells of the Cerebral Cortex. J. Neurosci. *34*, 11929–11947. 10.1523/JNEUROSCI.1860-14.2014.

26. Ishigame, H., Zenewicz, L.A., Sanjabi, S., Licona-Limón, P., Nakayama, M., Leonard, W.J., and Flavell, R.A. (2013). Excessive Th1 responses due to the absence of TGF-β signaling cause autoimmune diabetes and dysregulated Treg cell homeostasis. Proceedings of the National Academy of Sciences *110*, 6961–6966. 10.1073/pnas.1304498110.

27. Kisanuki, Y.Y., Hammer, R.E., Miyazaki, J., Williams, S.C., Richardson, J.A., and Yanagisawa, M. (2001). Tie2-Cre Transgenic Mice: A New Model for Endothelial Cell-Lineage Analysis in Vivo. Developmental Biology *230*, 230–242. 10.1006/dbio.2000.0106.

28. Foo, S.S., Turner, C.J., Adams, S., Compagni, A., Aubyn, D., Kogata, N., Lindblom, P., Shani, M., Zicha, D., and Adams, R.H. (2006). Ephrin-B2 Controls Cell Motility and Adhesion during Blood-Vessel-Wall Assembly. Cell *124*, 161–173. 10.1016/j.cell.2005.10.034.

29. Dickson, M.C., Martin, J.S., Cousins, F.M., Kulkarni, A.B., Karlsson, S., and Akhurst, R.J. (1995). Defective haematopoiesis and vasculogenesis in transforming growth factor-beta 1 knock out mice. Development *121*, 1845–1854. 10.1242/dev.121.6.1845.

30. Li, M.O., Wan, Y.Y., and Flavell, R.A. (2007). T Cell-Produced Transforming Growth Factor-β1 Controls T Cell Tolerance and Regulates Th1- and Th17-Cell Differentiation. Immunity *26*, 579–591. 10.1016/j.immuni.2007.03.014.

31. Yona, S., Kim, K.-W., Wolf, Y., Mildner, A., Varol, D., Breker, M., Strauss-Ayali, D., Viukov, S., Guilliams, M., Misharin, A., et al. (2013). Fate Mapping Reveals Origins and Dynamics of Monocytes and Tissue Macrophages under Homeostasis. Immunity *38*, 79–91. 10.1016/j.immuni.2012.12.001.

32. Matcovitch-Natan, O., Winter, D.R., Giladi, A., Vargas Aguilar, S., Spinrad, A., Sarrazin, S., Ben-Yehuda, H., David, E., Zelada González, F., Perrin, P., et al. (2016). Microglia development follows a stepwise program to regulate brain homeostasis. Science *353*, aad8670. 10.1126/science.aad8670.

33. Li, Q., Pangas, S.A., Jorgez, C.J., Graff, J.M., Weinstein, M., and Matzuk, M.M. (2008). Redundant Roles of SMAD2 and SMAD3 in Ovarian Granulosa Cells In Vivo. Mol Cell Biol *28*, 7001–7011. 10.1128/MCB.00732-08.

34. Ju, W., Ogawa, A., Heyer, J., Nierhof, D., Yu, L., Kucherlapati, R., Shafritz, D.A., and Böttinger, E.P. (2006). Deletion of Smad2 in Mouse Liver Reveals Novel Functions in Hepatocyte Growth and Differentiation. Mol Cell Biol *26*, 654–667. 10.1128/MCB.26.2.654-667.2006.

35. Li, Q., Cheng, Z., Zhou, L., Darmanis, S., Neff, N.F., Okamoto, J., Gulati, G., Bennett, M.L., Sun, L.O., Clarke, L.E., et al. (2019). Developmental Heterogeneity of Microglia and Brain Myeloid Cells Revealed by Deep Single-Cell RNA Sequencing. Neuron *101*, 207-223.e10. 10.1016/j.neuron.2018.12.006.

36. Keren-Shaul, H., Spinrad, A., Weiner, A., Matcovitch-Natan, O., Dvir-Szternfeld, R., Ulland, T.K., David, E., Baruch, K., Lara-Astaiso, D., Toth, B., et al. (2017). A Unique Microglia Type Associated with Restricting Development of Alzheimer's Disease. Cell *169*, 1276-1290.e17. 10.1016/j.cell.2017.05.018.

37. Krasemann, S., Madore, C., Cialic, R., Baufeld, C., Calcagno, N., El Fatimy, R., Beckers, L., O'Loughlin, E., Xu, Y., Fanek, Z., et al. (2017). The TREM2-APOE Pathway Drives the Transcriptional Phenotype of Dysfunctional Microglia in Neurodegenerative Diseases. Immunity *47*, 566-581.e9. 10.1016/j.immuni.2017.08.008.

38. Chytil, A., Magnuson, M.A., Wright, C.V.E., and Moses, H.L. (2002). Conditional inactivation of the TGF-? type II receptor using Cre:Lox. genesis *32*, 73–75. 10.1002/gene.10046.

39. Cunningham, C.L., Martínez-Cerdeño, V., and Noctor, S.C. (2013). Microglia Regulate the Number of Neural Precursor Cells in the Developing Cerebral Cortex. J Neurosci *33*, 4216–4233. 10.1523/JNEUROSCI.3441-12.2013.

40. Ginhoux, F., Greter, M., Leboeuf, M., Nandi, S., See, P., Gokhan, S., Mehler, M.F., Conway, S.J., Ng, L.G., Stanley, E.R., et al. (2010). Fate Mapping Analysis Reveals That Adult Microglia Derive from Primitive Macrophages. Science *330*, 841–845. 10.1126/science.1194637.

41. Masuda, T., Amann, L., Sankowski, R., Staszewski, O., Lenz, M., d´Errico, P., Snaidero, N., Costa Jordão, M.J., Böttcher, C., Kierdorf, K., et al. (2020). Novel Hexb-based tools for studying microglia in the CNS. Nat Immunol *21*, 802–815. 10.1038/s41590-020-0707-4.

42. McKinsey, G.L., Lizama, C.O., Keown-Lang, A.E., Niu, A., Santander, N., Larpthaveesarp, A., Chee, E., Gonzalez, F.F., and Arnold, T.D. (2020). A new genetic strategy for targeting microglia in development and disease. eLife *9*, e54590. 10.7554/eLife.54590.

43. Kaiser, T., and Feng, G. (2019). Tmem119-EGFP and Tmem119-CreERT2 Transgenic Mice for Labeling and Manipulating Microglia. eNeuro *6*, ENEURO.0448-18.2019. 10.1523/ENEURO.0448-18.2019.

44. Sheikh, B.N., Bondareva, O., Guhathakurta, S., Tsang, T.H., Sikora, K., Aizarani, N., Sagar, null, Holz, H., Grün, D., Hein, L., et al. (2019). Systematic Identification of Cell-Cell Communication Networks in the Developing Brain. iScience *21*, 273–287. 10.1016/j.isci.2019.10.026.

45. Yin, Z., Herron, S., Silveira, S., Kleemann, K., Gauthier, C., Mallah, D., Cheng, Y., Margeta, M.A., Pitts, K.M., Barry, J.-L., et al. (2023). Identification of a protective microglial state mediated by miR-155 and interferon-γ signaling in a mouse model of Alzheimer's disease. Nat Neurosci *26*, 1196–1207. 10.1038/s41593-023-01355-y.

46. Picelli, S., Björklund, Å.K., Faridani, O.R., Sagasser, S., Winberg, G., and Sandberg, R. (2013). Smart-seq2 for sensitive full-length transcriptome profiling in single cells. Nat Methods *10*, 1096–1098. 10.1038/nmeth.2639.

Supplemental Figure Legends

Supplemental Figure 1. Deletion of *Itgb8* in adulthood does not disrupt microglial homeostasis.
A) Expression analysis of *Itgb8* expression in adult astrocytes, neurons, oligodendrocytes, microglia, and endothelial cells[4]. **B)** *Itgb8* is expressed in oligodendrocytes (OLIG2+; PDGFRa+), OPCs (OLIG2+), astrocytes (SOX9, GFAP+/-), and neurons (NEUN+) in adulthood, as shown by immunohistochemical overlap with a *Itgb8-TdT* reporter line. **C)** Deletion of *Itgb8* using various cell-lineage restricted *Cre* and *CreER* mouse lines does not result in changes in motor behavior, unlike deletion with *Nestin-Cre*, which results in profound motor dysfunction. **D)** Deletion of *Itgb8* using various cell-lineage restricted *Cre* and *CreER* mouse lines does not result in changes in microglial homeostasis or associated astrocyte activation, unlike deletion with $Nestin^{Cre}$. Scale bars in B,D=100μm.

Supplemental Figure 2. Recombination analysis of *Cre* and *CreER* mouse lines used to delete *Itgb8*.
A) Cre-dependent nuclear GFP *Cre*-reporter line *SunTag* crossed to indicated *Cre* or *CreER* line, and brain sections from adult mice were stained for nuclear-localized markers of neurons (NEUN), oligodendrocytes and OPCs (OLIG2), or astrocytes (SOX9); images taken from motor cortex. **B)** Quantification of cell marker colocalization with SUN1GFP recombination report. 6 animals were quantified for $Nestin^{Cre}$ and $Olig2^{Cre}$, 4 for $Syn1^{Cre}$ and $Aldh1L1^{CreER}$ and 3 for $hGFAP^{Cre}$. 3 images per mouse were quantified from the cerebral cortex. Scale bar =100μm.

Supplemental Figure 3. Analysis of cell-type specific *Itgb8* expression. A) Single-cell RNA-seq analysis of *Itgb8* expression in the developing brain taken from [5]. Individual columns represent clustered categories of cell types. **B)** *Itgb8* in situ hybridization (ISH) at indicated time points taken from Allen Brain Atlas (https://mouse.brain-map.org). **C)** Analysis of *Itgb8-TdT* expression in E14.5 mouse brain stained for radial glia nuclei (SOX9, white) and radial glia processes (NESTIN, green). Scale bar in C=500μm.

Supplemental Figure 4. Cre-recombination and phenotypes in $Itgb8^{fl/fl};Olig2^{Cre}$ mice.
A) Coronal brain sections from indicated E14.5 mice stained for tdT (Cre recombination, red) and microglia/macrophages (IBA1, white); **B)** microglia (P2RY12 in green, see arrowheads) and immature macrophages (CD206 in magenta); **C)** hemorrhage (red blood cells marked by TER119 in red and vascular endothelium marked by CD31 in blue); tdT (red) and **D)** apical progenitors (SOX9, green). Note lack of recombination of apical progenitors and also lack of microglia or vascular/hemorrhage phenotypes in these mice. Scale bar in A=150μm, scale bar in B= 100μm.

Supplemental Figure 5. Gene ontology and transcriptional analysis of TGFβ mutant models.
A-B) Gene ontology analysis of **A)** sorted microglia and **B)** bulk-Seq from different TGFβ mutant models. Putative genes involved in differential neuromotor phenotypes in TGFβ mutants were selected based on differential expression in distinct mouse models. Overrepresentation analysis was performed in each set separately as indicated by respective colors. **C)** Expression changes of genes driving enrichment of selected GO terms. Levels are shown as Log_2FoldChange for microglia and whole brain from all analyzed mutants. We selected processes likely to be important in microglia-associated neuromotor impairments (i.e. regulation of phagocytosis, Toll-like receptor gene family and signaling, synaptic pruning, and myelination). Color scales are distinct for microglia and whole brain.

Supplemental Figure 6. Epistatic analysis of *ApoE* contribution to the *TgfbR2* conditional mutant microglial phenotype.
A) Diagram describing potential pathway interaction between upregulated ApoE in the *Tgfbr2* conditional mutant model and the downstream MGnD/DAM microglial phenotype. **B)** Analysis of effect of simultaneous deletion of *ApoE* and microglial *TgfbR2*. No change was seen in $ApoE^{+/-}$; $TgfR2^{fl/+};Cx3cr1^{Cre}$ *versus* $ApoE^{-/-}$; $TgfR2^{fl/+};Cx3cr1^{Cre}$ in dysmature morphology, P2RY12 expression loss, CD206 upregulation. Scale bar in B=100μm. Scale bar in B=25μm for higher magnification image.

Figure 1: Deletion of *Itgb8* in early embryonic radial glia disrupts microglial maturation.

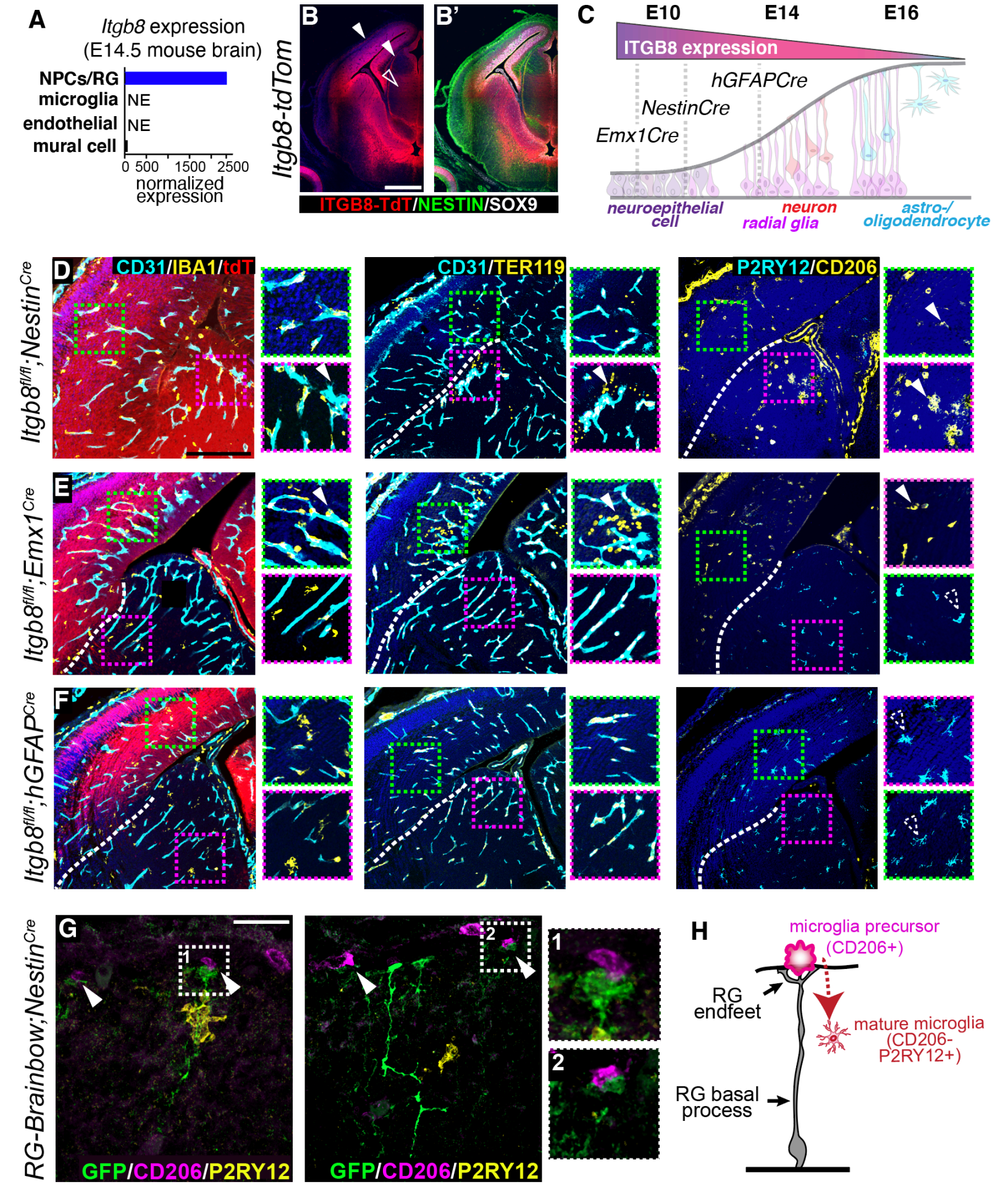

Figure 2: *Emx1-Cre* deletion of *Itgb8* results in anatomically restricted blockage of microglial differentiation.

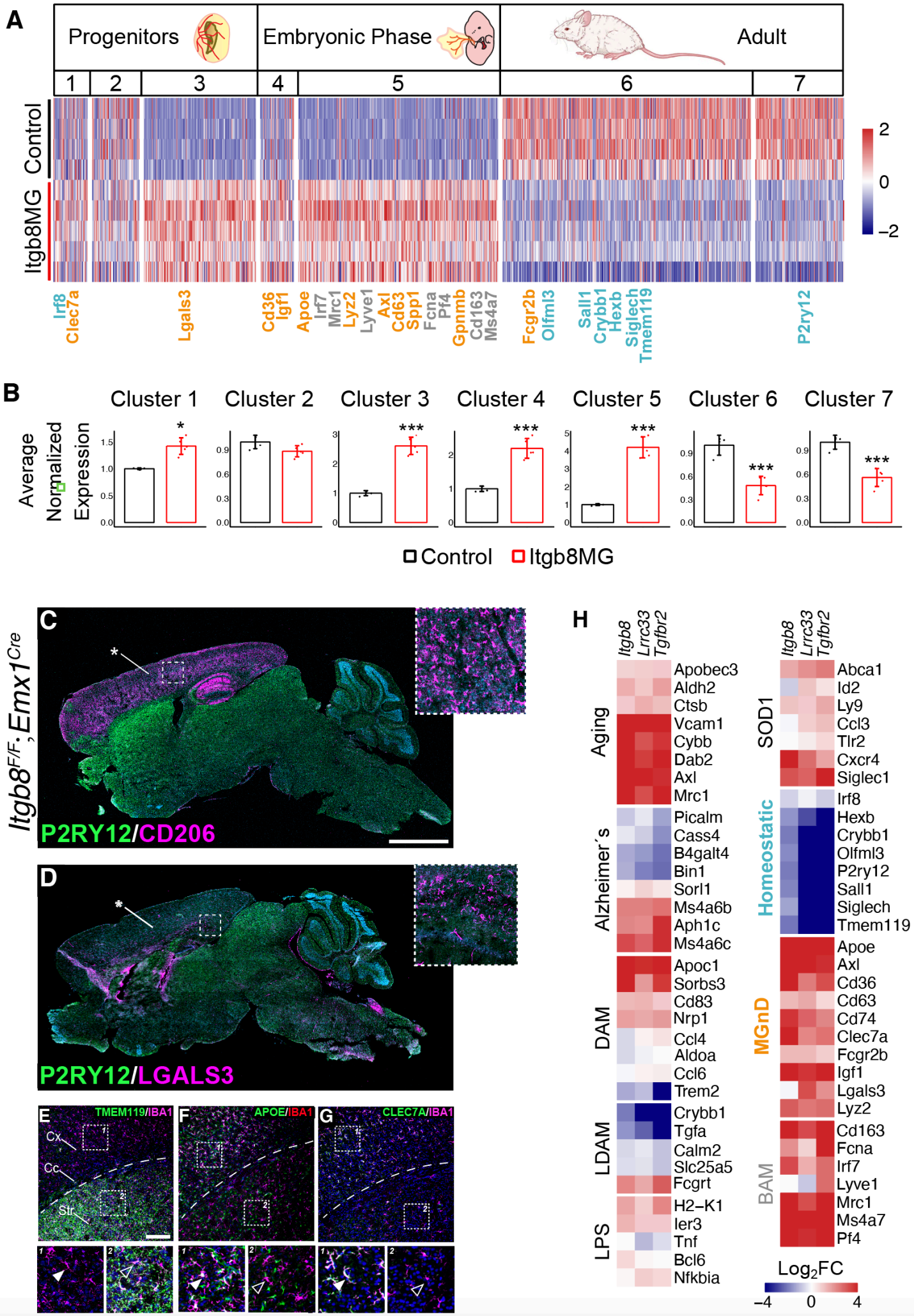

Figure 3: Microglial dysmaturation due to *Tgfb1* deletion in microglia/macrophages.

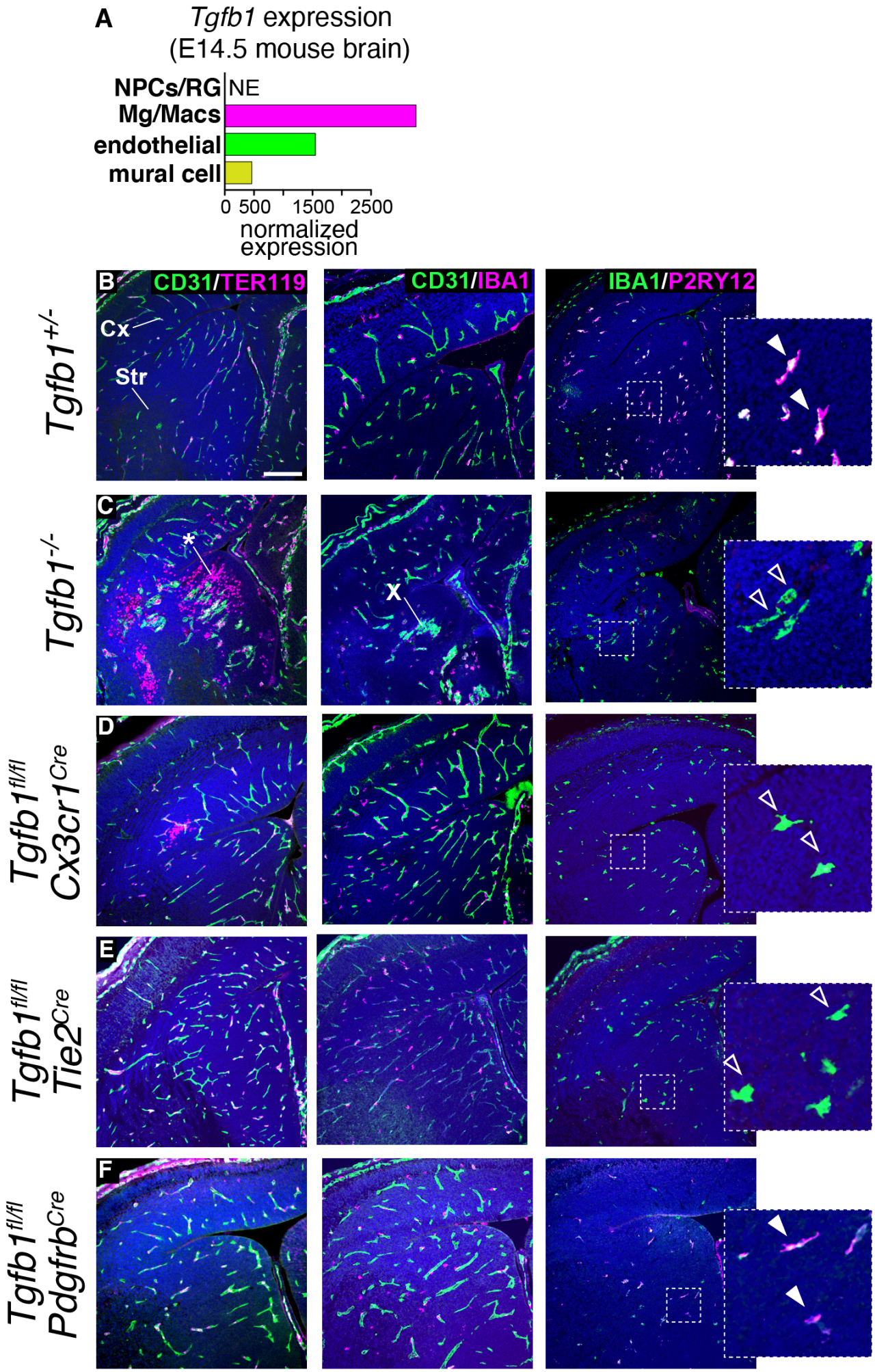

Figure 4: Microglia provide their own TGFB1 to promote and maintain homeostasis.

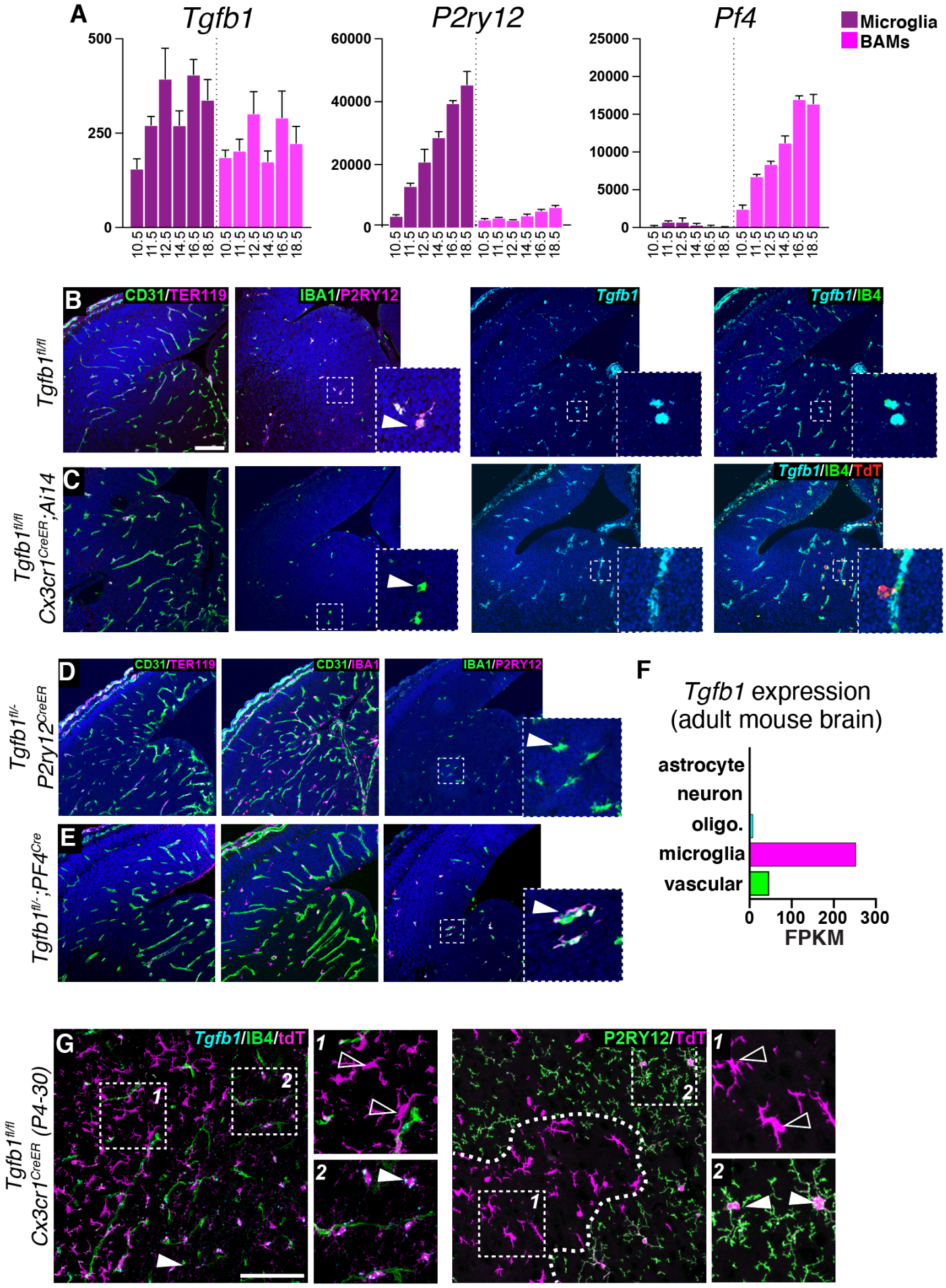

Figure 5. Disruption of non-canonical TGFβ signaling in microglia drives disease-associated gene expression.

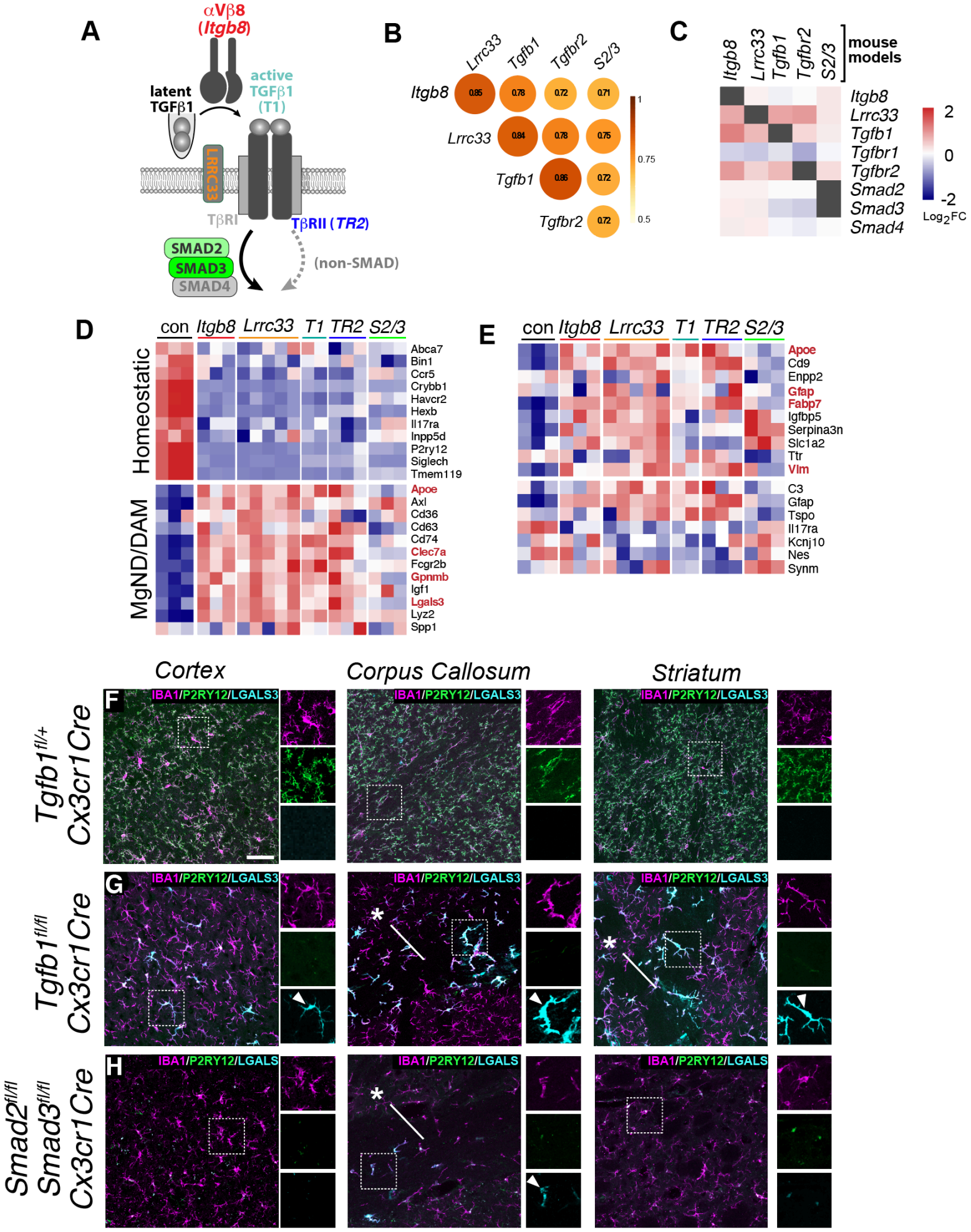

Supplemental Figure 1: Deletion of *Itgb8* in adulthood does not disrupt microglial homeostasis.

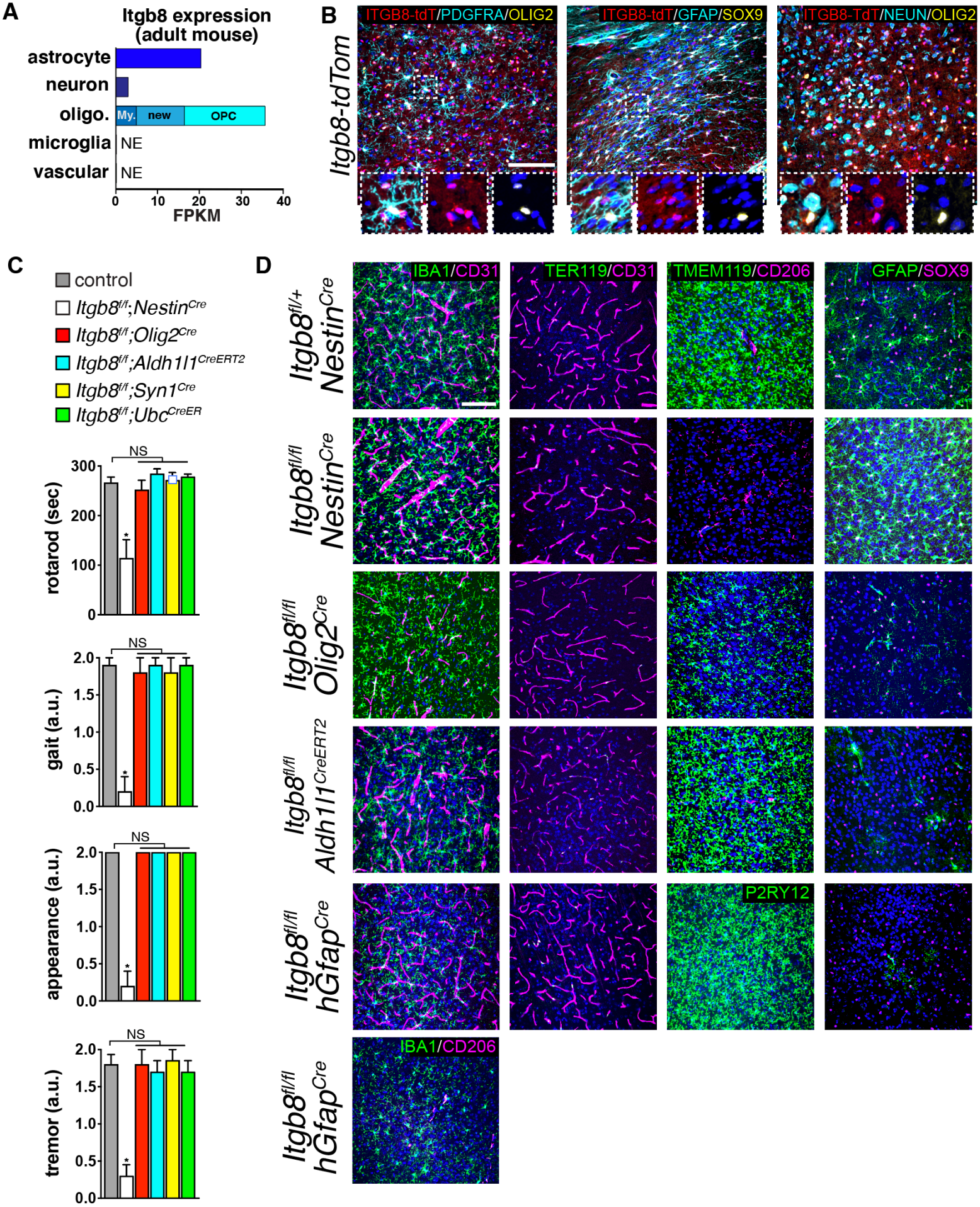

Supplementary Figure 2: Recombination analysis of *Cre* and *CreER* mouse lines used to delete *Itgb8*.

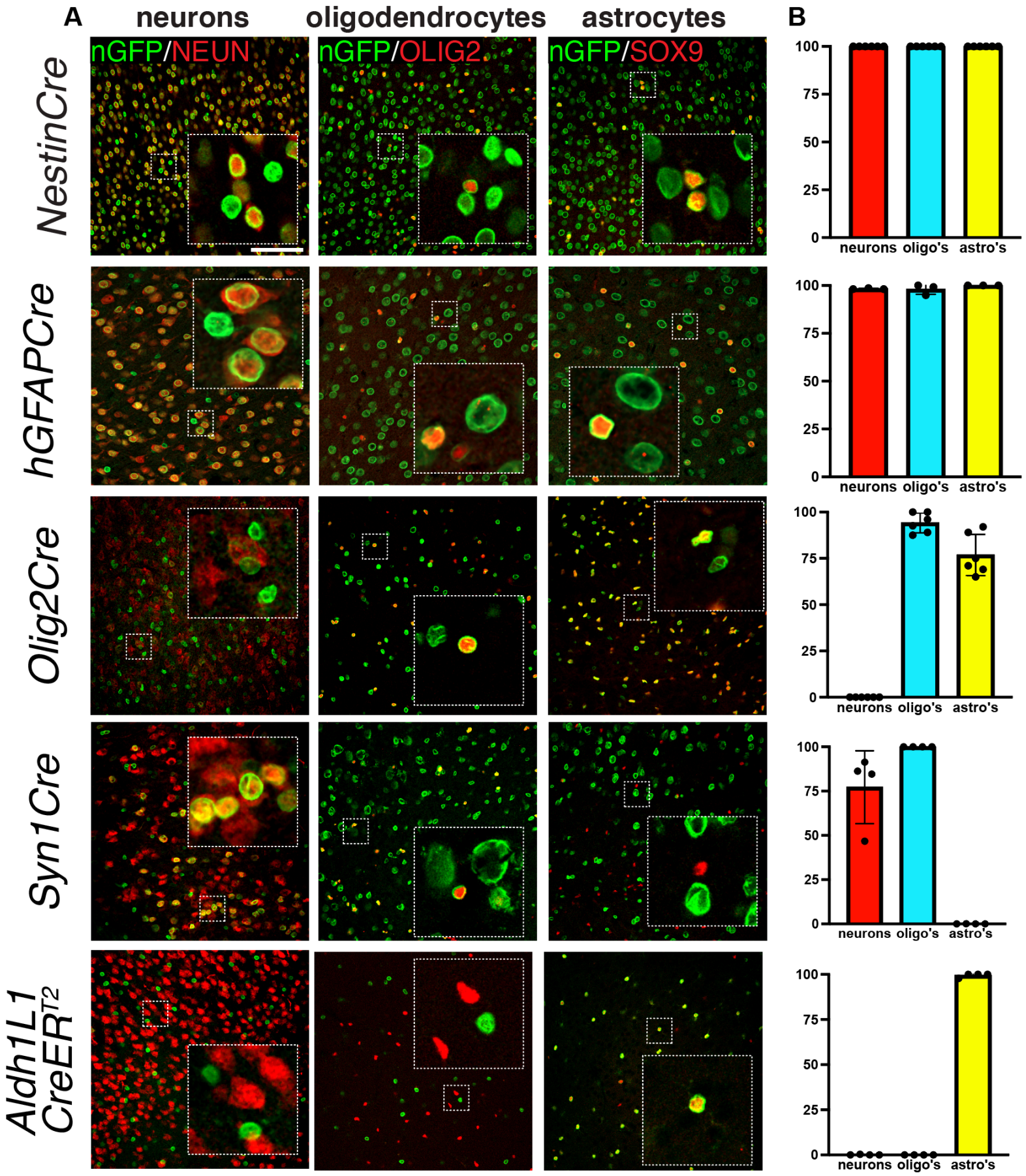

Supplemental Figure 3: Analysis of cell-type specific *Itgb8* expression.

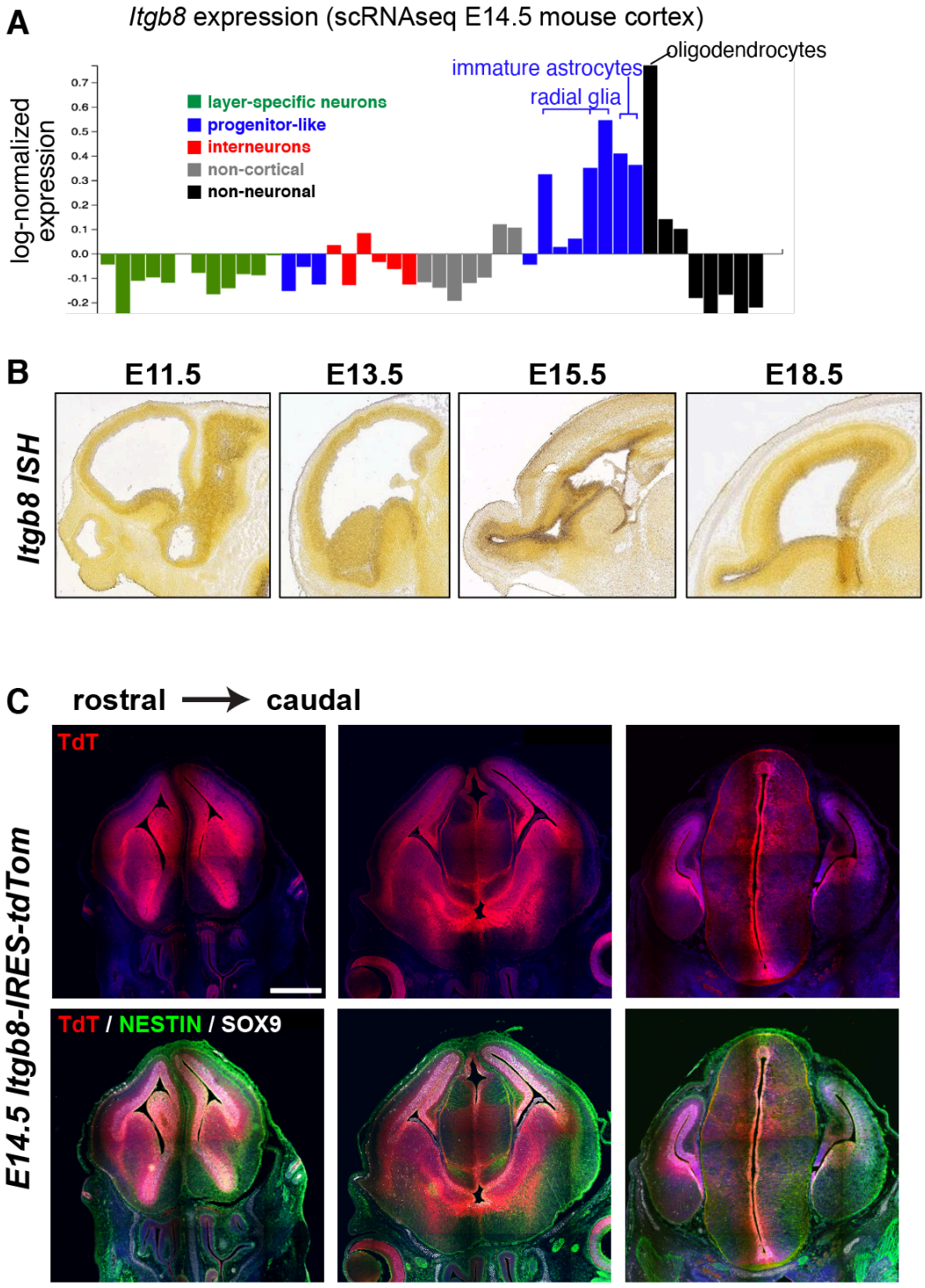

Supplemental Figure 4: Cre-recombination and phenotypes in *Itgb8fl/fl;Olig2Cre* mice.

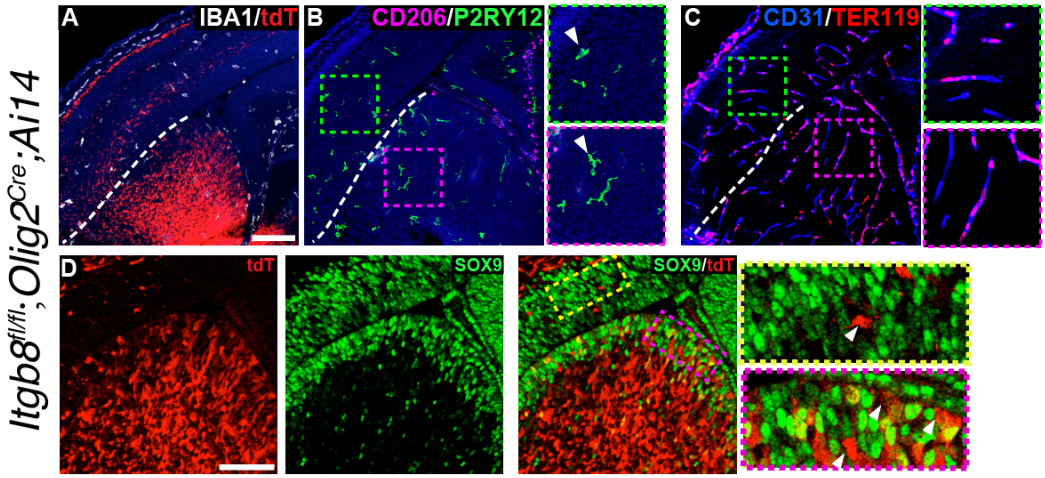

Supplemental Figure 5: Gene ontology and transcriptional analysis of TGFβ mutant models.

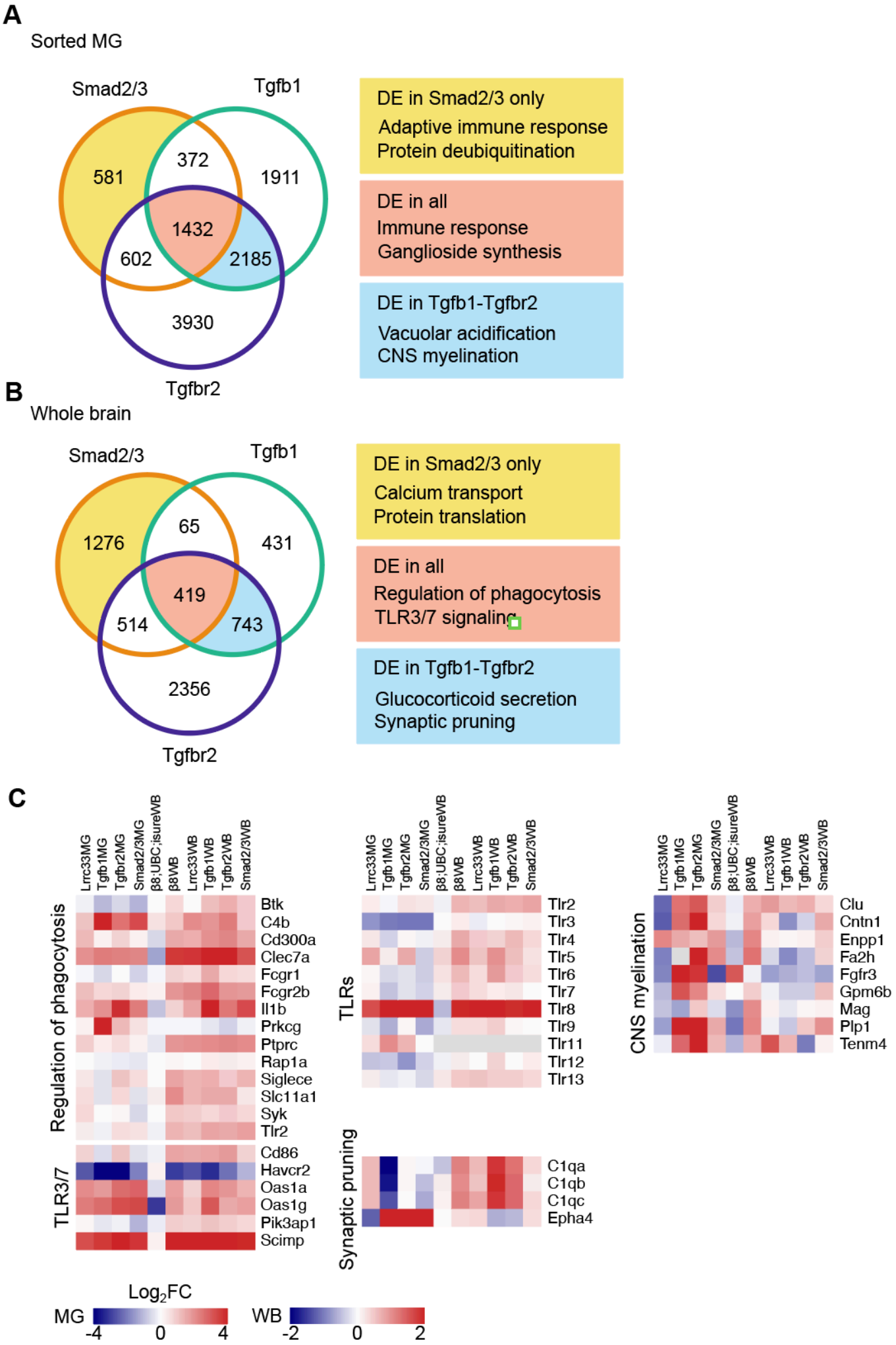
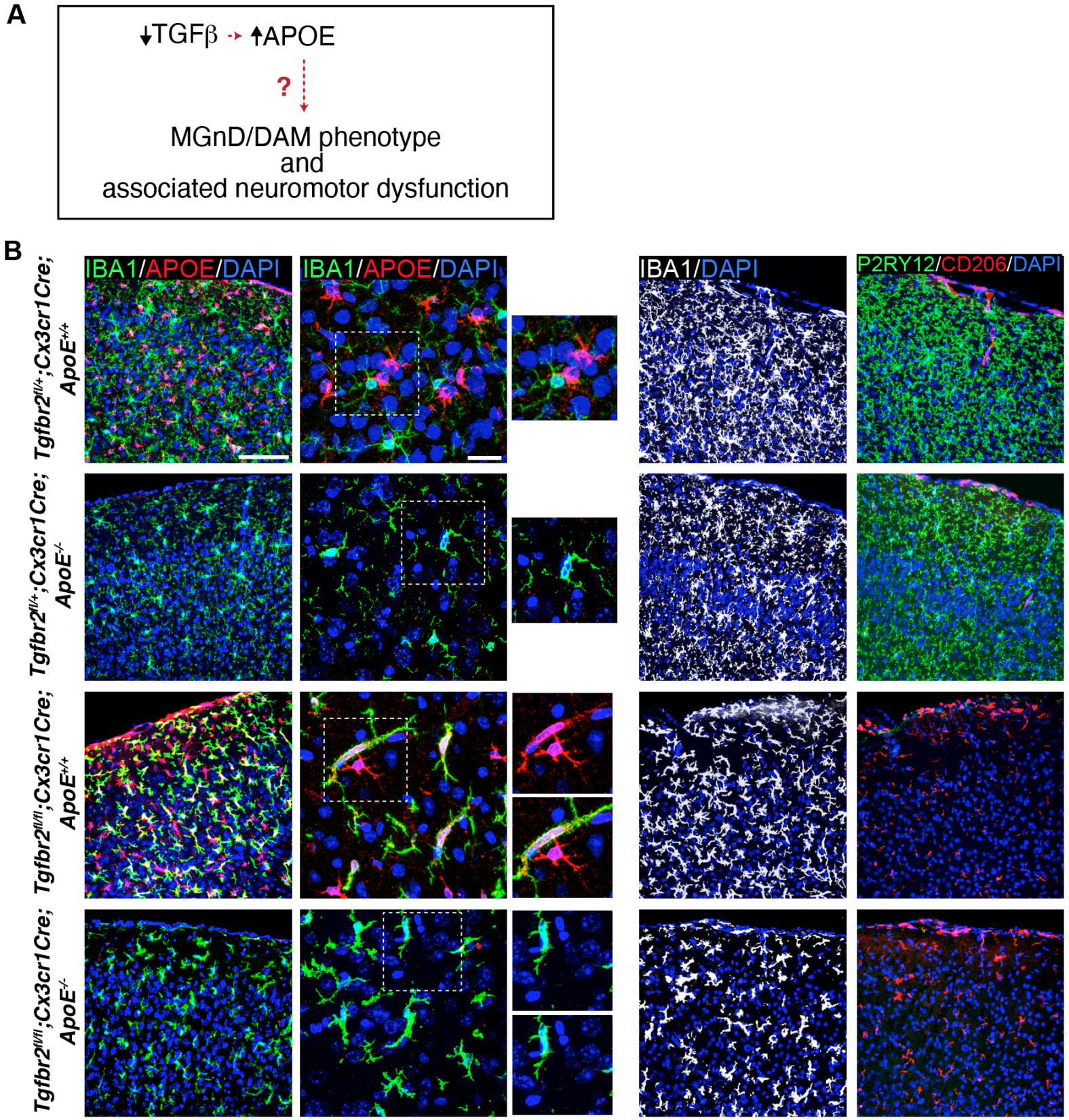
Supplemental Figure 6: Epistatic analysis of *ApoE* contribution to the *TgfbR2* conditional mutant microglial phenotype.